UNIVERSITAT POLITÈCNICA DE CATALUNYA
BARCELONATECH

Escola Tècnica Superior d'Enginyeria
de Telecomunicació de Barcelona

Analysis of electrode arrays for multichannel surface electromyography

A Master's Thesis

Submitted to the Faculty of the

Escola Tècnica d'Enginyeria de Telecomunicació de Barcelona

Universitat Politècnica de Catalunya

by

Eduard Pérez Obiols

In partial fulfilment

of the requirements for the degree of

MASTER IN ELECTRONICS ENGINEERING

Advisor: Miguel Angel Mañanas / Juan Ramos

Barcelona, May 2019

Title of the thesis: **Analysis of electrode arrays for multichannel surface electromyography**

Author: Eduard Pérez

Advisor: Miguel Angel Mañanas, Mislav Jordanic, Juan Ramos

Abstract

Nowadays medical evaluation requires in each further step improvements in all the areas concerning engineering and materials. This applies to the application of electromyography and in specific to surface electromyography which is being used every day to evaluate muscular and neuromuscular diseases. In this field electrodes are used as interfaces to acquire the biopotential signals generated by muscles. The materials usually used in these electrodes are expensive. This fact can be a limitation factor for the applications that use a considerable number of them such as High Density surface electromyography.

This thesis aims to evaluate using tests, parameters extraction, results analysis and performance comparison a set of different electrode arrays in order to evaluate the suitability of low cost material specifically stainless steel to perform the same tasks as other materials used in medical applications such silver or silver chloride electrodes.

I dedicate this thesis to my parents, uncles and my grandma. On the other hand I dedicate it to Natalia for all the time giving me her support and encouraging me to get the best out of me, thank you all.

Acknowledgements

I would like to thank the people from CREB who has helped me to elaborate this thesis and to allow me to use their material and facilities. I want to thank also the people who volunteered as subjects of this thesis.

Special thanks to my advisors Miguel Angel Mañanas and Mislav Jordanic for the guidance in the development of this thesis, the effort, the support and the patience with me.

I want to thank and acknowledge Erica Triviño for the work done.

Finally, I would like to thank Juan Ramos for being my coadvisor.

Revision history and approval record

Revision	Date	Purpose
0	27/01/2019	Document creation
1	18/02/2019	Document update
2	08/03/2019	Document revision and update 1
3	10/04/2019	Document revision 2

Written by:		Reviewed and approved by:	
Date	27/01/2019	Date	14/05/2019
Name	Eduard Pérez	Name	Miguel Angel Mañanas
Position	Project Author	Position	Project Supervisor

Table of contents

Abstract 1
Acknowledgements 3
Revision history and approval record 4
Table of contents 5
List of Figures 7
List of Tables 9
1. Introduction 10
2. Objectives 14
2.1. Main objective 14
2.2. Specific objective 14
3. Methodology 15
3.1. Electrode arrays 15
3.1.1. Materials 15
3.1.2. The pattern 16
3.1.3. Electrode substrate 17
3.1.4. Electrical interface 17
3.1.5. Prototypes 18
3.2. Recording protocol 20
3.2.1. Equipment 20
3.2.2. Subjects 22
3.2.3. Protocol 22
3.2.4. Set up 25
3.3. Signal Processing 26
3.3.1. Preprocessing 27
3.3.2. Extraction of EMG measures 27
4. Results and Discussion 34
4.1. Time signals 34
4.1.1. Time series graphs, ... 35
4.1.2. Time series results 41
4.2. Signal Spectra 42
4.2.1. Spectra graphs 42
4.2.2. Spectra graphs, separate channels 45

4.2.3. Signal spectra results 49
4.3. Bivariate analysis 49
4.3.1. Bivariate analysis graphs 51
4.3.2. Bivariate analysis results 55
4.4. Intensity analysis 56
4.4.1. Intensity analysis graphs 56
4.4.2. Intensity analysis results 58
4.5. Boxplots of Conduction Velocity (CV) 59
4.5.1. Boxplots of Conduction Velocity graphs 60
4.5.2. Boxplots of Conduction Velocity results 68
4.6. Regression coefficients 69
4.6.1. Regression coefficients results. 70
5. Conclusions and future development 72
Bibliography 74
Appendices 76

List of Figures

Figure 1: Two motor units, motor neurons and muscular fibers (Strang 2013) 10
Figure 2: EMG Mathematical model (Basmajian and De Luca 1985) 11
Figure 3: Silver electrode 15
Figure 4: Silver chloride electrode 15
Figure 5: Stainless steel electrode 15
Figure 6: Array pattern 16
Figure 7: Electrical interface 17
Figure 8: Adapter and electrode wire 18
Figure 9: Desktop Amplifier cable with connector 18
Figure 10: Adaptor / connector junction of a desktop amplifier cable 18
Figure 11: Electrode soldered adaptor 18
Figure 12: Silver array prototype 19
Figure 13: Stainless steel prototype 19
Figure 14: Silver chloride array prototype 19
Figure 15: Silver array from BIOART group 20
Figure 16: Wireless multichannel amplifier 20
Figure 17: HDMI amplifier adaptor 21
Figure 18: EMG desktop amplifier 21
Figure 19: Tools used in exercise recording 22
Figure 20: Exercise Set up 25
Figure 21: Array pattern 26
Figure 22: Exercise defined parts 28
Figure 23: Windowing and segments processing 29
Figure 24: Time signal 1, Silver, 50% MVC 35
Figure 25: Time signal 2, Silver, 50% MVC 36
Figure 26: Time signal 3, Silver, 30% MVC 36
Figure 27: Time signal 4, Silver, 30% MVC 37
Figure 28: Time signal 5, Silver, 10% MVC 37
Figure 29: Time signal 6, Silver, 10% MVC 38
Figure 30: Time signal 7, Stainless steel, 50% MVC 38
Figure 31: Time signal 8, Stainless steel, 50% MVC 39
Figure 32: Time signal 9, Stainless steel, 30% MVC 39

Figure 33: Time signal 10, Stainless steel, 30% MVC 40
Figure 34: Time signal 11, Stainless steel, 10% MVC 40
Figure 35: Time signal 12, Stainless steel, 10% MVC 41
Figure 36: Spectrum Silver 50% MVC 42
Figure 37: Spectrum Stainless steel 50% MVC 43
Figure 38: Spectrum Silver 30% MVC 43
Figure 39: Spectrum Stainless steel 30% MVC 44
Figure 40: Spectrum Silver 10% MVC 44
Figure 41: Spectrum Stainless steel 10% MVC 45
Figure 42: Scatter plot showing Correlation coefficient and CV 49
Figure 43: Bivariate graph Correlation coefficient /CV 50
Figure 44: Bivariate analysis Silver SD 51
Figure 45: Bivariate analysis Silver DD 52
Figure 46: Bivariate analysis Stainless steel SD 53
Figure 47: Bivariate analysis Stainless steel DD 54
Figure 48: Intensity analysis, Boxplot 1 56
Figure 49: Intensity analysis, Boxplot 2 57
Figure 50: Intensity analysis, Boxplot 3 57
Figure 51: Intensity analysis, Boxplot 4, all subjects 58
Figure 52: Conduction Velocity boxplot 100% MVC SD 60
Figure 53: Conduction Velocity boxplot 100% MVC DD 61
Figure 54: Conduction Velocity boxplot 10% MVC SD 62
Figure 55: Conduction Velocity boxplot 10% MVC DD 63
Figure 56: Conduction Velocity boxplot 30% MVC SD 64
Figure 57: Conduction Velocity boxplot 30% MVC DD 65
Figure 58: Conduction Velocity boxplot 50% MVC SD 66
Figure 59: Conduction Velocity boxplot 50% MVC DD 67
Figure 60: Regression coefficient, MDF 69
Figure 61: Regression coefficient, MNF 69
Figure 62: Regression coefficient, CV 70
Figure 63: Regression coefficient, RMS 70

List of Tables

Table 1: Exercise set 24

1. Introduction

Motivation

In the context of medical diagnosis, muscular afflictions and illnesses are a common problem regarding the locomotor system. Muscular disorders, nerve disorders and other problems affecting the connection between nerves and muscles including as examples muscular dystrophy, myasthenia gravis, radiculopathies or carpal tunnel syndrome need to be diagnosed (Danielle Moores and Erica Cirino 2016).

The electromyographic signal (EMG) represents the recording of the electric potential generated by the muscle fiber membrane depolarization during the contraction of a muscle (Merletti and Farina 2016). Muscles are consisted of muscle fibers which are innervated and controlled by neurons. Muscle fibers are cells with stable difference of intracellular and extracellular potential in resting state. During the contraction, neural signal triggers the depolarization of a muscle fiber, which then spreads along muscle the fiber and causes the contraction. This depolarization is called muscle fiber action potential and can be measured as a difference in potential between two electrodes. To maximize the amplitude of recorded signal, the electrodes should be positioned along the direction of the muscle fiber. Each neuron triggers multiple muscle fibers simultaneously. Therefore, a motor neuron and all muscle fibers that it innervates are called muscle unit, whereas the recorded depolarization signal is called muscle unit action potential (MUAP).

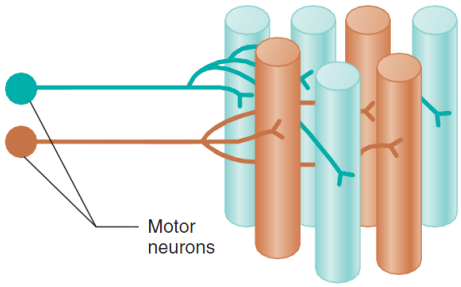

Figure 1: Two motor units, motor neurons and muscular fibers (Strang 2013)

In a resting state, there is an approximate constant voltage of -90 mV between the inside and the outside of the muscle fiber. This potential is called Rest Membrane Potential (RMP). The depolarization of a muscular fiber turns the RMP to approximately +10 mV. The spread of this depolarization is called fiber action potential. Conduction velocity refers to the velocity at which this action potential moves over the membrane.

This parameter helps in the measurement of fatigue of the muscle as it has an inverse relationship with it.

Muscle fatigue can be defined as a loss of the ability to produce force with the muscle. It is the result of prolonged or repetitive works (DeLuca 1984).

There are two main types of electromyographic measurements: the intramuscular EMG and the surface EMG (sEMG).

The intramuscular EMG consists of introducing an electrode by means of a needle into the body. It is an invasive measuring method which allows the positioning of the recording electrodes in very close proximity of the muscle fibers. This type of recording ensures a very selective recording of muscle fibers in close proximity of electrodes and is characterized by high signal to noise ratio, but will not be considered in this thesis.

Surface electromyography (sEMG), on the other hand is a technique that even though it shares common objective with electromyography, it uses a different approach. In surface electromyography, the electrode is located outside of the body and over the skin. The signal acquired this way represents the recording of many different muscular fibers. The characteristics of recorded EMG signal at a given moment depends on the properties of muscle fibers, number of active muscle units and their firing frequency, distance and impedance between the muscle unit and electrodes, and orientation of electrodes with respect to muscle fibers. Therefore, EMG can mathematically be modeled as a superposition of recorded MUAPs at a given time, as illustrated in the Figure 2.

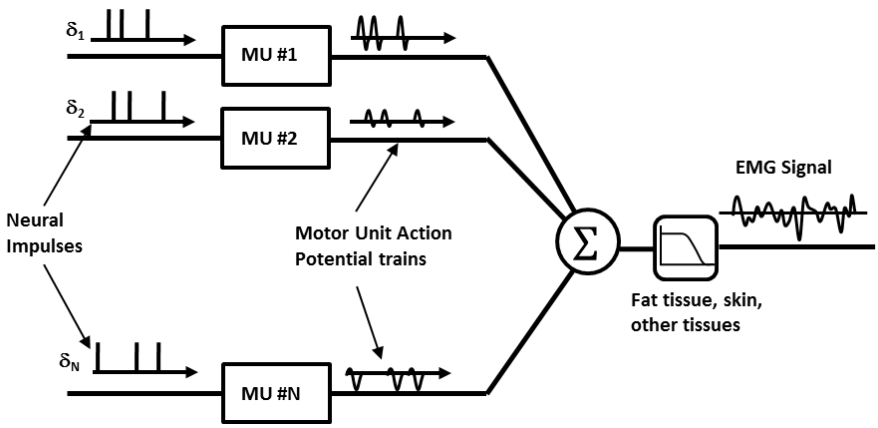

Figure 2: EMG Mathematical model (Basmajian and De Luca 1985)

The following equation describes the generation of sEMG signal:

$$sEMG(t) = \sum_{i=1}^{N} \sum_{j=-\infty}^{+\infty} MUAP_i(t) \cdot \delta\left(t - t_{i,j}\right) + n(t)$$

, where N is the number of motor units, $MUAP_i(t)$ is the waveform of action potential of i^{th} motor unit as recorded at the electrodes, $t_{i,j}$ is the time of firing of i^{th} motor neuron, and $n(t)$ describes the additive noise.

The sEMG signals can be acquired using both monopolar and bipolar (also known as single differential) configurations. Monopolar approach records the actual surface potential with respect to the reference electrode, which is not located over the muscle of interest. The drawback is that it also records interference sources and

other muscle activity sources that are not meant to be recorded, phenomenon known as crosstalk. On the other hand, the single differential configuration measures the difference of potential between two closely spaced electrodes and is able to reduce the interference as it appears in similar amplitude on consecutive electrodes. The level of attenuation of the interference depends on CMRR (Common mode rejection ratio), which is a parameter of the amplifier, and similarity of the two electrode-skin impedances. The drawbacks are the reduction in the detection volume and the attenuation of the deeper potential contributions of the muscle (Cavalcanti Garcia and Vieira 2011).

With technological development in the field of microelectronics and increase of transistor density in silicon, recently it became possible to record high number of EMG channels simultaneously. These advancements introduced multichannel EMG recording. By collocating multiple recording electrodes over the skin covering the muscle, it is possible to extract more precise and valuable information about the neuromuscular activity. There are two types of multichannel EMG sensing arrays with respect to the pattern in which electrodes are located in the array: linear electrode arrays, and high-density EMG electrode arrays. In linear electrode arrays, the electrodes are collocated in a single line (normally with inter-electrode distance from 0.5 cm to 2 cm) and during the recording the array is positioned along the direction of muscle fibers. This configuration enables monitoring of propagation of MUAPs, calculating the conduction velocity of muscle fibers, and localization of innervation zone, i.e., the location in the muscle where neuron innervates muscle fibers (Ashley- Ross 2005). All these parameters have valuable clinical applications.

Even more information can be extracted by recording high-density surface electromyography (HD-sEMG). By positioning the electrodes in two-dimensional grid it is possible to extract the information on spatial distribution of myoelectric activity over the muscle surface, and therefore the distribution of active motor units within the muscle. It was already proven that spatial distribution of EMG activity changes in dependence of exerted force, joint angle, and fatigue (Staudenmann et al. 2013; Vieira, Merletti, and Mesin 2010).

Moreover, it was demonstrated that recorded HD-EMG signal can be decomposed into individual firings of muscle units, which is proportional to neural train that controls the muscle (Figure 1). That is, by using the decomposition algorithm, the neural code can be extracted non-invasively from EMG signal (Holobar et al. 2010; Holobar and Zazula 2007).

The historical evolution of EMG starts in 18th century and is closely associated with the discovery of electricity. It is not until 20th century that the evolution in technology allowed the precise amplification and recording of biopotentials. The first steps were done by physiologists, later on neurologists contributed by linking electrophysiological findings with clinical and pathological significance. The World War II period helped the progress significantly due the large amount of patients with nerve injuries (Kazamel and Warren 2017). Nowadays, EMG devices are used daily in rehabilitation centers and hospitals for therapy and rehabilitation, in control of exoskeletons (Vaca Benitez et al. 2013), prosthetic (Li, Schultz, and Kuiken 2010) and orthotic devices, control of rehabilitation robots (Marchal-Crespo and

Reinkensmeyer 2009) and virtual reality systems, but also in gamification (Van Dijk et al. 2016), leisure, and sports (Verikas et al. 2016).

Usually the interface to record the signals are pairs of electrodes in bipolar configuration although other interfaces like arrays of electrodes may be used as well in high density surface electromyography (HD-sEMG). The common materials of the electrodes are silver/silver chloride (Ag/AgCl), silver (Ag) and gold (Au).

The first ones (Ag/AgCl) are preferred as they are almost non-polarizable and that makes them less sensitive to motion artifact besides provide a highly stable interface with the skin when electrolyte solution is applied between the electrode and the skin (Cavalcanti Garcia and Vieira 2011).

These materials are expensive and nowadays researchers are trying to find and test new materials with a lower associated cost.

In this thesis, three type of electrodes are tested and compared with focus on their performance:

- Brass electrodes with silver-plated surface (referred to as “silver” in the rest of the thesis)
- Silver / silver chloride electrodes
- Medical grade stainless steel electrodes

The 2D recording arrays were manufactured using these electrodes and HD-EMG was recorded on biceps brachii muscle. From the recorded signals conduction velocity, fatigue indexes, and signal-to-noise ratio were calculated and analyzed in terms of repeatability and quality of estimation.

2. Objectives

2.1. Main objective

This thesis addresses the problem of finding a low-cost and easy-to-use alternative for electrode material in HD-EMG sensing array. The objective of the thesis is to compare and evaluate three electrode arrays used for EMG recording without application of conductive gel in terms of EMG signal quality parameters and robustness of extracted physiological parameters.

2.2. Specific objective

Considering the main objective, a set of specific objectives is defined:

- To develop three electrode arrays for HD-EMG recording. This includes 1) selecting the materials for three electrode arrays, 2) manufacturing the arrays, and 3) verifying that signals can be effectively acquired and recorded.
- To evaluate, adjust, and select the appropriate devices of the acquisition system from several available options
- To develop and prepare a protocol for recording the EMG signal database
- To record the signal database in a set of subjects
- To process the recorded signals and extract descriptive measures of signal quality
- To analyze and compare the electrode arrays in terms of the extracted measures

3. Methodology

3.1. Electrode arrays

3.1.1. Materials

The first step to develop the arrays was to choose the materials that were going to be evaluated. The selected ones were:

- Silver-plated brass electrode, diameter: 6 mm

Figure 3: Silver electrode

- Silver / silver chloride, diameter: 4 mm

Figure 4: Silver chloride electrode

- Stainless steel, diameter: 6mm

Figure 5: Stainless steel electrode

The first two are common interface materials in electrode manufacturing due to the electrical properties. The last one is the material that had to be tested with respect to the others. The selection in this case was motivated by the significantly lower price with respect the other two electrode materials.

3.1.2. The pattern

Several patterns or distribution of electrodes can be used to develop an array. Since there are some constraints the possible solutions are restricted. The constraints are the following ones:

- Fixed inter-electrode distance (IED) is needed. This constraint allows us later to compute parameters as the conduction velocity (CV).
- A maximum and minimum muscle area that the prototype has to cover.
- The electrodes should not overlap, otherwise the connections could short.
- The electrodes should have an area big enough to get a minimum quality level of signal. There is a trade-off between the third constraint and this one.

All these constraints led us to a possible solution that is a squared pattern with equispaced electrodes in it.

The selected dimension is 5 x 4 electrodes with an IED of 10 mm

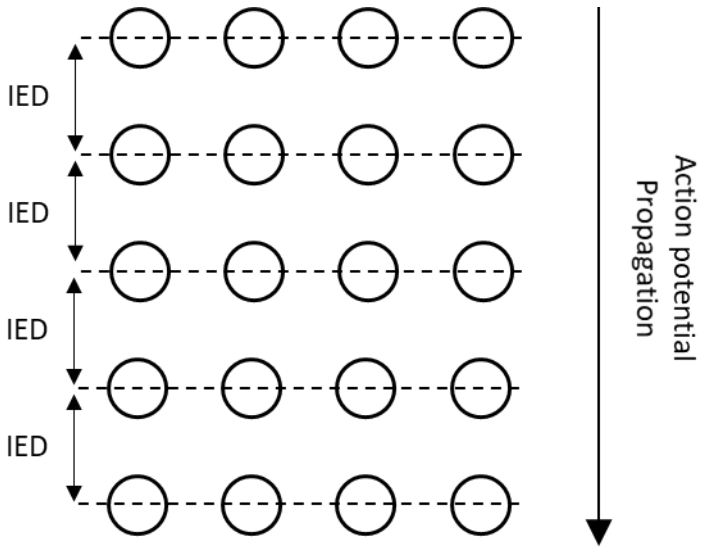

Figure 6: Array pattern

3.1.3. Electrode substrate

The substrate in which the electrodes needed to be embedded had to be flexible to accommodate different muscle contours, robust to allow the device to be used multiple times, breathable to minimize perspiration which can change electrode-skin impedance and even short-circuit adjacent electrodes, non-stretchable to keep the inter-electrode distance between electrodes fixed. As a straightforward and functional solution we used a cotton fabric.

3.1.4. Electrical interface

Each array was connected through wires to an interface that was later connected to the desktop amplifier. The connections were done by soldering. In the case of stainless steel, the surface of the electrodes was treated with hydrochloric acid prior to soldering.

The connectors of the desktop amplifier used during the recording had a unique order of EMG channels. Therefore, special attention was needed in order to match the exact pinout of the connectors in the electrode array prototypes.

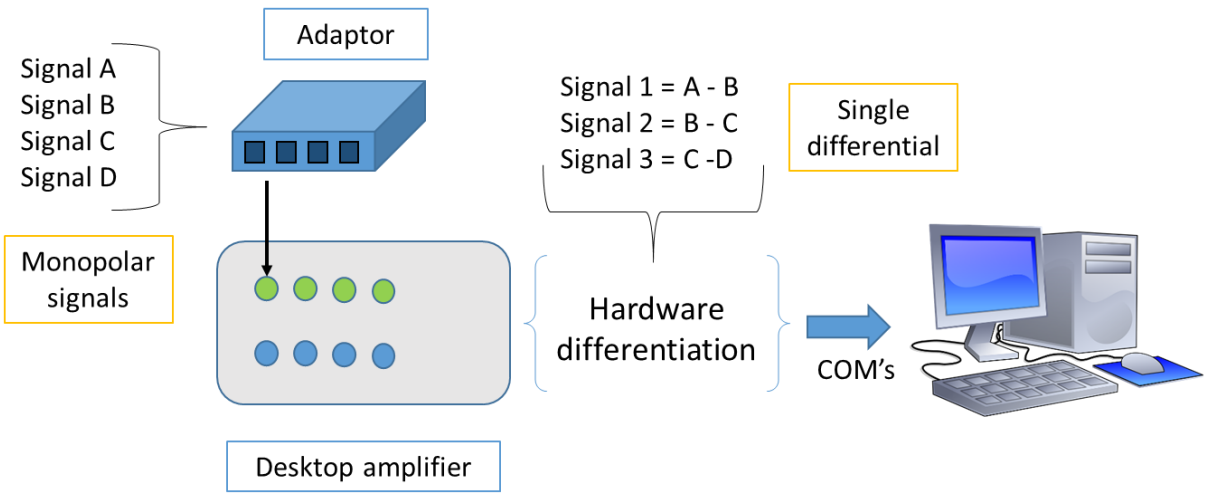

Figure 7: Electrical interface

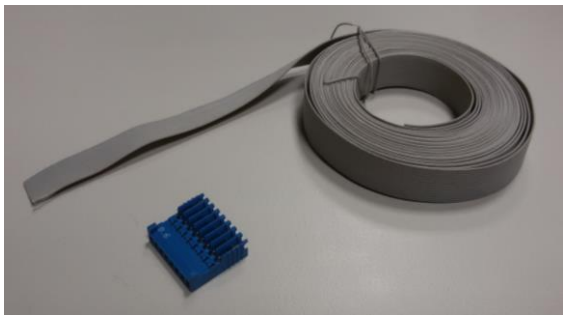

Figure 8: Adapter and electrode wire

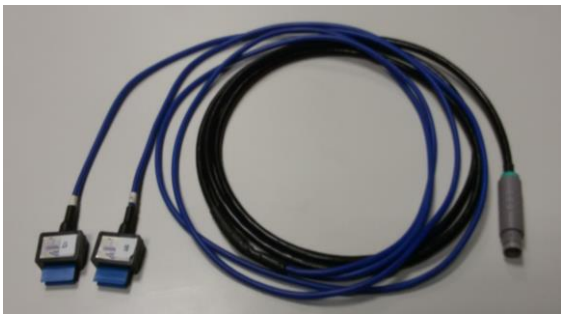

Figure 9: Desktop Amplifier cable with connector

Figure 10: Adaptor / connector junction of a desktop amplifier cable

Figure 11: Electrode soldered adaptor

3.1.5. Prototypes

To attach the array to subject's body, a strap was needed. The strap was done by sewing velcro bands to the fabric. The length should accommodate a variety of diameters so the extreme values must assure a good positioning of the array in all subjects.

During the first tests with silver chloride array prototype (Figure 14) it was noticed that the silver chloride array due to the electrodes and the final set-up up would not last and resist enough time. Although some results were acquired and processed, the array was discarded and another array with embedded silver-plated eyelets, previously developed in the BIOART research group (the group where this thesis was carried out), was used (Figure 15).

Figure 12: Silver array prototype

Figure 13: Stainless steel prototype

Figure 14: Silver chloride array prototype

Figure 15: Silver array from BIOART group

3.2. Recording protocol

3.2.1. Equipment

The equipment used during the recording was divided in two groups. The first is the equipment regarding the acquisition system and the environment used to collect the data.

1. Acquisition system, tools and computer

The initial idea was to use a wireless multichannel amplifier developed previously in the BIOART lab. The amplifier was integrated in a box together with the necessary circuitry, battery and an implemented firmware to communicate with the PC using a Wi-Fi antenna.

Figure 16: Wireless multichannel amplifier

The input channels to this amplifier were HDMI connectors. In order to be able to connect the arrays an adaptor was designed and manufactured.

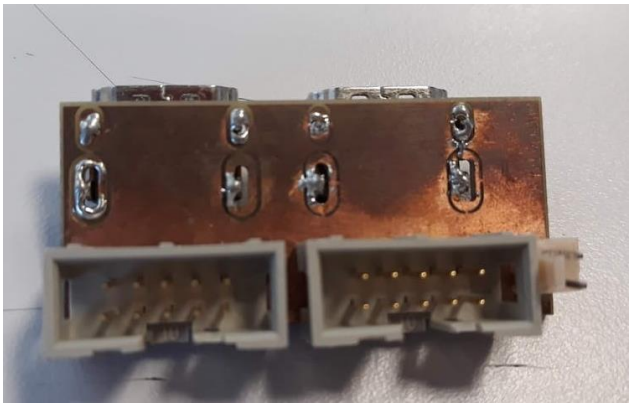

Figure 17: HDMI amplifier adaptor

By doing the first attempts to record signal with the PC, it was discovered that parts of the received signal were missing. By doing additional tests, the problem was associated with antenna and the casing of the device. As it was not possible to assure the proper function of the device, this recording option was discarded.

The proposed alternative option was the EMG desktop amplifier with 128 channels available in the lab.

Figure 18: EMG desktop amplifier

The device is intended for multichannel surface electromyography amplification. It allows simultaneous acquisition, amplification, filtering and recording up to 128 channels with a sampling frequency of 2048 Hz and to register single differential channels together with the software OT Biolab. Each of the 8 sockets can manage inputs up to 16 channels coming from a cable connected to the electrodes. Regarding the security, this device has a medical grade electrical insulation of all

the circuitry connected to the subject. The device is a research instrument for clinical purposes and not available for general use.

2. Tools used in each exercise of the protocol

During the exercise, the following equipment was used: rope, a dynamometer, a timer and a chair.

Moreover, the following auxiliary tools were also used: gauze, gel, isopropyl alcohol and water to clean and prepare the skin, step pipette and electrical ground wristband.

Figure 19: Tools used in exercise recording

3.2.2. Subjects

The subjects were asked to voluntarily contribute to this work and were recruited both from the same group and other groups from Escola Tècnica Superior d'Enginyeria Industrial de Barcelona (ETSEIB). In order to accomplish with the confidential aspects, the anonymity shall be preserved referring to them as subjects or subject # for individual approach. In total there were nine people, in the range between 21 and 35 years old, eight male and one female.

3.2.3. Protocol

The protocol that has been designed consists of four exercises. Between each exercise a rest time is defined also.

For each array the same set of four exercises was carried out.

The sequence in which each array is recorded in each subject was randomized to avoid, correlations derived from the same order

First, the skin needed to be prepared. There are different ways to approach this cleaning (Merletti and Farina 2016):

1. No treatment
2. **Rubbing with ethyl alcohol**
3. Rubbing with abrasive paste
4. Stripping with adhesive tape
5. Washing with soap (30 sec) and rinsing

The second option was used because of the improvement with respect to not treating the skin, the facility to acquire and apply the material and the lack of materials as abrasive paste.

First step was to clean the area where the array was going to be put on with a gaze and alcohol to remove oily substances.

As the alcohol leaves the skin very dry and does not improve its conductance a second step with a wet gaze was applied, that helped to reduce the electrode-skin impedance (Cavalcanti Garcia and Vieira 2011).

Before each exercise started, a blank time of 5 seconds with the setup prepared to begin but with no contraction of the muscle was recorded in order to acquire signal in which all the sources except the muscular activity itself were recorded - mainly noise and interferences. Later, these recordings would help to compute the SNR of the channels.

The exercise consists of an isometric contraction of the biceps brachii during a specified time. This is done by pulling a rope connected to a dynamometer to measure the exerted force while an assistant provided a verbal feedback to the subject. During the exercise, the force had to be kept as constant as possible to ensure isometric contraction.

In each consecutive exercise, a fraction of the maximal voluntary contraction (MVC) was defined as a target force. The first exercise set the reference for the rest of exercises by applying the maximum voluntary contraction and hence the maximum force.

i. Exercise 1
   The subject was supposed to develop the 100% of its MVC and was important that this applied force was kept constant until the end of a specified period of 10 seconds. The force was monitored using the dynamometer.

ii. Exercise 2
This exercise consisted in applying the 10% MVC. The reference was used to estimate the corresponding force by computing the weight to pull. For example, if 20 kg were pulled in the first exercise, in the second exercise the subject was supposed to pull 2 kg (10%).

iii. Exercise 3
The third exercise consisted in apply the 30% of MVC. The weight to pull was computed in the same manner as in exercise 2.

iv. Exercise 4
The last exercise was 50% of the MVC and, contrary to the rest of the exercises, it lasted for 2 minutes or until subject could not maintain the constant level of force further. During this exercise, muscle fatigue developed.

The scheme for the exercises is summarized in the following table.

Total time	**Action**	**Notes**	**Time**
	Skin preparation		
00:00	Exercise 1	100% MVC	10 s + 5 s
00:15	Rest		2 min
02:15	Exercise 2	10% MVC	10 s + 5 s
02:30	Rest		1 min
03:15	Exercise 3	30% MVC	10 s + 5 s
03:30	Rest		2 min
05:30	Exercise 4	50% MVC	Up to 2 min + 5s
	End		

Table 1: Exercise set

3.2.4. Set up

The purpose of the posture shown in (Figure 20) is to help the subject to activate just the biceps brachii.

The set up used to record each exercise is shown. As it can be seen, the rope had a dynamometer in one side to measure the force applied and a hand taken in the other side. The elbow had to keep contact with a surface.

Figure 20: Exercise Set up

Each subject was instructed to maintain the same posture during the contraction and to perform the exercise by activating only biceps brachii muscle.

The arm and the position of the array was the same during all the exercises.

While the subject sat and the skin was being prepared, an assistant was taking care to control the chronometer in order to meet the times and rests for each exercise, as defined in table 1.

3.3. Signal Processing

Before describing the processing, itself, relevant information shall be exposed:

- 20 electrodes were used in each array.
- The signals were acquired in single differential mode; differentiation was done at the hardware level. The final number of channels then (using 20 electrodes) is 16 and this is due to the configuration in four columns and five rows each (Figure 21). When positioned to the body, the columns were aligned with the propagation of muscle unit action potentials.

  There were 5 electrodes in each column (same color in Figure 21). In each column (propagation direction), differential signals between consecutive electrodes were measured. The signals acquired at the PC level were:

  - Starting with the first column (red) the differential signals between the following electrodes were recorded, 1 - 2, 2 - 3, 3 - 4, 4 – 5. Although the differential signal between last electrode (5) in first column (red) and first electrode (1) in second column (blue) 5 – 1 was also acquired, this one was discarded as it does not preserve the IED. Four differential signals were acquired in each of four columns, having a total of 16 differential signals.

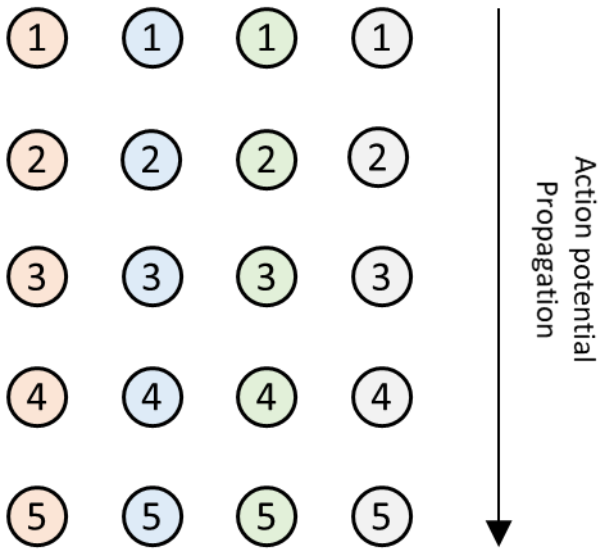

Figure 21: Array pattern

- The sampling frequency of the system was 2048 samples/second.
- The software to gather the signals was OT BioLab by OT Bioeletronica linked with the acquisition hardware.
- The software used to process the signals was Matlab by Mathworks.

3.3.1. Preprocessing

Before starting to extract measures the signal was filtered:

- Band pass filtering: Signals were filtered using a zero-phase (filtfilt matlab function) flat frequency response, 3rd order Butterworth filter with cut-off frequencies of 15 Hz and 350 Hz. This is approximately the bandwidth range of EMG reference.
- Notch filtering: 50 Hz is filtered due to its large contribution of power-line interference. Despite some authors (Luca 2002) (Day 2004) recommend not to filter this frequency because it is in the EMG bandwidth, in most of the signals processed in this work the filter is applied, the third harmonic, 150 Hz, is also filtered. The filters applied have a central frequency of 50 and 150 Hz respectively with a bandwidth of 2 Hz. The functions used to implement them are iirnotch Matlab function to calculate the coefficients and filtfilt function to apply them to the data.

3.3.2. Extraction of EMG measures

In this section, the parameters and implemented algorithms to process the samples are explained.

The parameters computed are:

SNR (dB): Signal to noise ratio. This parameter is computed for each channel and measures the ratio between signal power and noise power. This parameter when measured experimentally is done under two assumptions:

-Power measurement of noise assumes no useful signal is in that measurement, and the measurement of signal power assumes useful signal is much larger than the noise contribution. To depict and explain better the parameter a signal recording divided in parts follows:

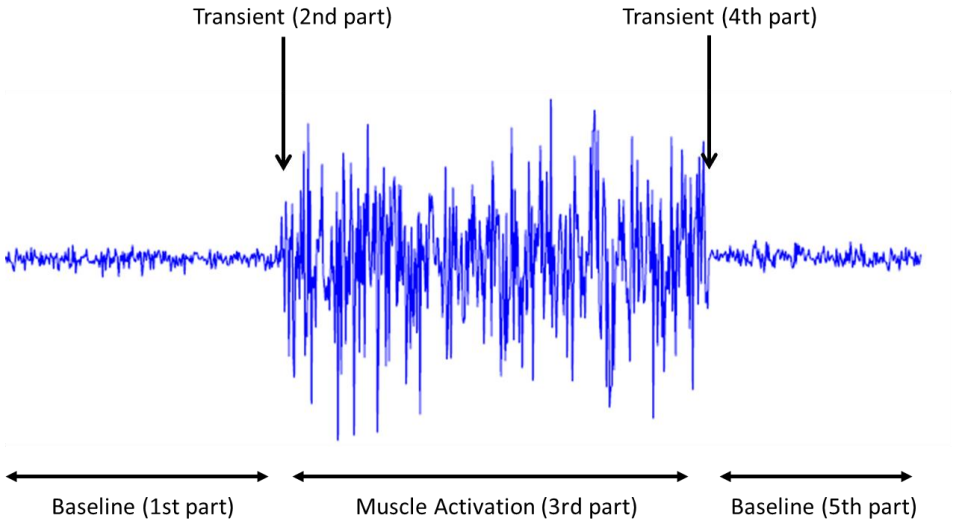

Figure 22: Exercise defined parts

The SNR compares the power of the signal gathered in the first part (noise power) and the power of the signal gathered in the third part (useful signal).

$$SNR_{dB} = 10 \cdot \log \frac{P_{signal}}{P_{noise}}$$

Considerations in this part:

- We avoid the use of transitory parts (2nd and 4th part) as the power is not constant.
- We have to take into account that as we have used the assumption of a much higher contribution of the useful signal in the power estimation of useful signal (3rd part), the confidence of this measure has a dependency on the exercise done (percentage of MVC). Different percentages of MVC give different amplitudes and different powers comparing the same signal part among exercises.
- As it is described in (Merletti and Farina 2016), when the electrode is placed over the skin the contact makes at some point the skin sweat. This sweating has an impact on the electrode skin impedance decreasing it and helping therefore to couple the electrode.

R: Cross Correlation. This parameter measures the degree of similarity of two time signals. related are in each time step.

$$R_{xy}(\tau) = \int_{-\infty}^{\infty} x(t+\tau) y^*(t) dt$$

This measure between two signals allows:

- Quantify how related are two signals, correlation coefficient (magnitude)
- Make out if its positive or negative relation, correlation coefficient (sign)
- Search for the highest correlation (peak in cross correlation function) between this two signals when shifting in time.
- If the correlation coefficient is high enough understand the time associated to this peak as a time shift (τ) between alike time signals

The correlation is computed between each pair of consecutive differential signals in one column of the array.

At this point is important to highlight the way the signal is going to be analyzed.

First in each array there are 20 electrodes divided in columns of 5 electrodes, so 4 single differential signals per column, a total of 16 signals.

The following procedure is explained focusing on just one single differential signal but is applied to all of them.

1. The signal is windowed in segments of 500 ms, first segment comprises first 500 ms.
2. The window is shifted for a step of 250 ms comprising from time 250 ms to 750 ms, 500 ms in total but overlapping the first segment a 50% of the samples.
3. The window goes forward 250 ms more so third segment goes from 500 ms to 1000 ms, 500 ms in total and overlapping a 50% with the second segment,
4. From this point, step 2 is repeated until the end of the recording is reached

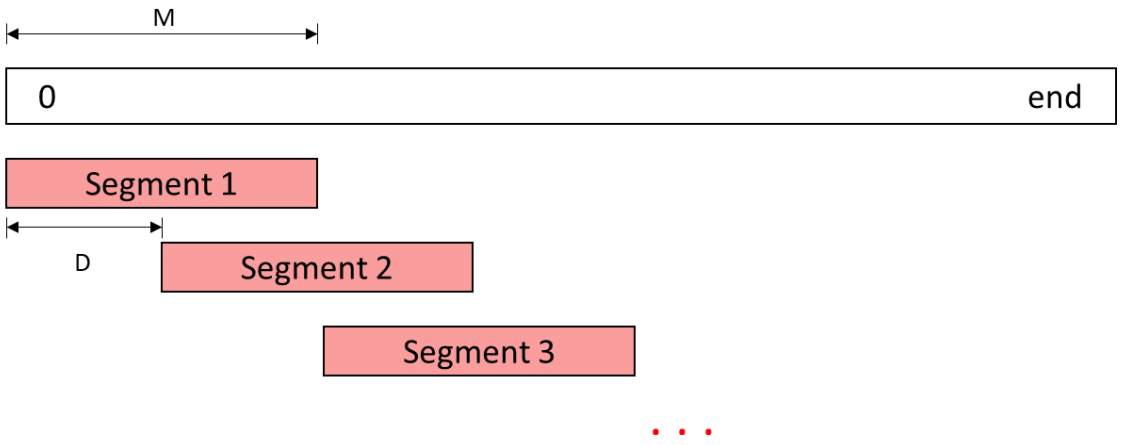

Figure 23: Windowing and segments processing

M = Length of the Windows = 500 ms
D = Step of the window = 250 ms

CV (m/s): Conduction Velocity. Physical parameter that reflects the propagation velocity of the depolarization potential over the membrane in the muscle fiber.

$$CV = \frac{IED}{Phase\ shift}$$

IED represents the inter-electrode distance and measures 10 mm, whereas Phase shift represents the time shift existing among the two differential signals used to derive this parameter. As explained before if the maximum of the correlation function is high enough indicates a great similarity between signals and the time associated to the moment at which the signals are more alike understood as a time shift. This time shift determines how much time the signal needs to propagate from location of one electrode to the other (separated by IED), and describes the conduction velocity (CV). As the system is discrete, the time shift is given in number of samples instead of actual time. This values are acquired from the cross-correlation function.

MNF (Hz): Mean Frequency. MNF is a frequency-domain feature that is usually used to assess muscle fatigue. It is defined by the average frequency calculated by summing the products of EMG power spectrum bins and dividing by the sum of the power spectrum bins. (Limsakul et al. 2012)

$$MNF = \sum_{j=1}^{M} f_j \cdot P_j \Big/ \sum_{j=1}^{M} P_j$$

f_j: frequency value of EMG power spectrum bin j.

P_j: EMG power spectrum at the frequency bin j.

M: Number of frequency bins.

MDF(Hz): Median Frequency. MDF is a frequency-domain feature that is also used to assess muscle fatigue. It is defined as the frequency at which the EMG power spectrum is divided in two regions with the equal power at both sides, the frequency that splits the power spectrum in two regions with same area. (Asghari Oskoei, Hu, and Gan 2009)

$$\sum_{j=1}^{MDF} P_j = \sum_{MDF}^{M} P_j = \frac{1}{2}\sum_{j=1}^{M} P_j$$

Because of the skewness of the EMG power spectrum the MNF is always slightly higher than MDF.(Knaflitz, Merletti, and De Luca 2017)

The evaluation and appreciation of muscle fatigue using surface EMG comprises several techniques as it can be RMS or averaged instantaneous frequency but MNF and MDF parameters have been accepted as one of the best solutions due the fact that a muscle fatigue manifests as a shift of the EMG spectrum towards the lower frequencies. (Petrofsky, Glaser, and Phillips 1982)

The parameters MNF and MDF were calculated from the power spectrum estimate of EMG signal. The method used for this estimation was Welch-Bartlett method due to reduction of the variance by averaging periodograms of the time signal segments (Manolakis, Ingle, and Kogon 2000).

At this point the processing of the signal is approached. Starting by the SNR the parameters estimation algorithms are explained and discussed, whereas the algorithm implementation can be found in the appendix.

Signal to Noise Ratio (SNR)

Even though a time is defined for each exercise, the recordings were performed manually and therefore differences exist in the starting time of the muscle activation in each recording. That is why an automated way to set the starting time of muscle activation is not reliable. Instead, the following steps were performed:

- Every recording was visually inspected
- Starting time of muscle activation and ending time (if existing) were observed
- The times were written in a text file associated to each recording
- The text file was used later in the Matlab script to process the SNR together with the rest of parameters

These times correspond in (Figure 22) as the transients. (2^{nd} and 4^{th} parts) In order to avoid parts with non-constant power, a margin of 512 samples corresponding to 250 ms is kept when computing both power of noise and power of signal.

Conduction Velocity (CV)

For the CV estimation, the segments of two consecutive channels were used. With the computation of this parameter, a problem appeared. As the CV makes use of the phase shift between this two segments, the sampling frequency limited the resolution.

The conduction velocity range of human muscles is between 3 m/s and 5 m/s approximately (Merletti and Farina 2016). With an IED of 10 mm and a sampling frequency of 2048 samples/second the result is a highly quantized CV and this makes extremely difficult to detect trends or slopes in the CV function.

As increase of the sampling frequency needs to be considerable, a solution was to once the correlation was computed it was interpolated with the purpose to add samples and then increase the resolution of the CV. The equation that explains considers the interpolation factor follows:

$$CV = \frac{IED}{Phase\ shift / IF}.$$

IF: Interpolation factor

F_s: Sampling Frequency

The phase shift in a discrete signal is given by a number of samples (integer quantity). When the signal is interpolated the number of samples is increased by the interpolation factor and the phase shift accordingly. Therefore, to represent a shift in time the phase shift needs to be normalized (divided) by the interpolation factor.

As a result, in the equation of CV, the denominator is a fraction instead of an integer. The resolution increases with the interpolation factor but there is a limit in the amount of samples that can be interpolated in a reliable way. The other solution to increase further more the resolution (reduce the quantization effect in CV, not temporal resolution) would be increasing the sampling frequency.

It can be noticed that finer changes in the denominator turn into finer changes (less quantized) in the CV.

Mean Frequency (MNF)

The computation of the MNF was an exact translation of the equation that defines the parameter performed individually to each channel. Starting from the estimated EMG spectrum the addition of the multiplication of the frequency bins by the power contained in each bin having as a result this spectral descriptor.

Median Frequency (MDF)

For the computation of the MDF, the following procedure was used:

- Sum all the bins of the power spectrum to know the total value of the spectrum → P_{sum}
- Compute the cumulative function of the bins of the power spectrum → $P_{cumulative}$
- Find the first frequency such that:

$$P_{cumulative} \geq \frac{P_{sum}}{2}$$

- The frequency bin that by addition to the cumulative function accomplishes the inequality is the estimated median frequency MDF.

4. Results and Discussion

In this section first the results and then the discussion is going to be presented.

In order to do it a list of meaningful ways to represent data follows:

- Time signals
- Signal Spectra
- Bivariate Analysis
- Intensity comparison
- Boxplots
- Regression coefficients

While performing the tests as it has been explained earlier in this work the third electrode array broke and another one from BIOART group was used. This array appears in the results with the name “reference”, since it was previously used in various successful research projects by the group.

The results and discussion section is focused and mainly emphasizes the result with the silver array and stainless steel array, although the same tests were performed with the BIOART group array using gel and not using gel as well.

4.1. Time signals

In this section, segments of time signal are presented. These figures show the best representative time segments those that have a higher correlation coefficient. The purpose of this time signal representations is to observe the quality of the signals by visual inspection. Some points to consider are:

- The correct visualization of the channels depicted
- The observation of the motor unit action potential (MUAP)
- The propagation of the MUAP along channels and time
- Check that high correlations are not due to power line couplings
- Check for non-expected behavior of the segments considered

In each figure are represented first a title with the subject who it belongs to if it was a dry test (not using gel) or with gel applied previously to the electrodes (some recordings were performed with gel in the case of the silver array from BIOART group to look for differences in the results of that specific array the focus, however, is in the dry results between silver array prototype and stainless steel prototype), the name of the material, the percentage of maximal voluntary contraction (MVC), and the column of the array which this signal was recorded from (1 to 4).

The main upper graph shows 200 ms of the four differential signals recorded from one column of the array. The selection criterion of the column was the higher averaged correlation coefficient among all the columns. The averaged correlation coefficient was calculated averaging the three correlation coefficients resulting from each pair of consecutive differential signals in a column, this correlation coefficient appears on top of the graph.

Below the single differential graph, it is depicted a double differential (differential signal of two differential signals) graph corresponding to the ordered differentiation of the signals in the single differential graph, i.e., double differential signals in the same time window. On top of this one there are the results of the estimation of CV using double differential signals, as there are three double differential signals two CVs are estimated, they are represented in (m/s).

There are two figures per material and MVC percentage, not taking into account the 100% MVC.

4.1.1. Time series graphs,

Material: Silver, 50% MVC

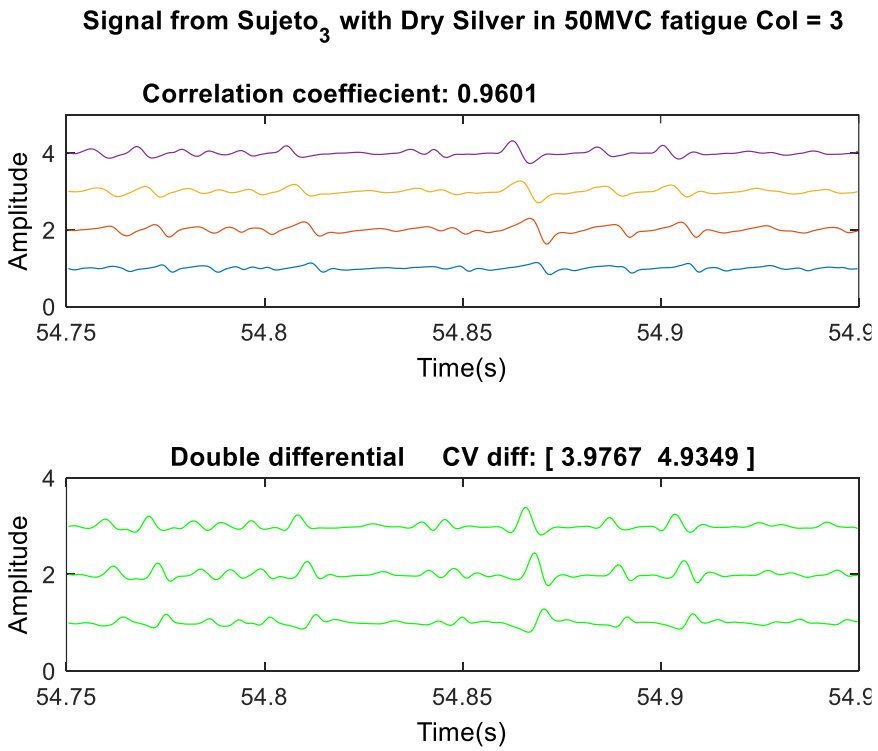

Figure 24: Time signal 1, Silver, 50% MVC

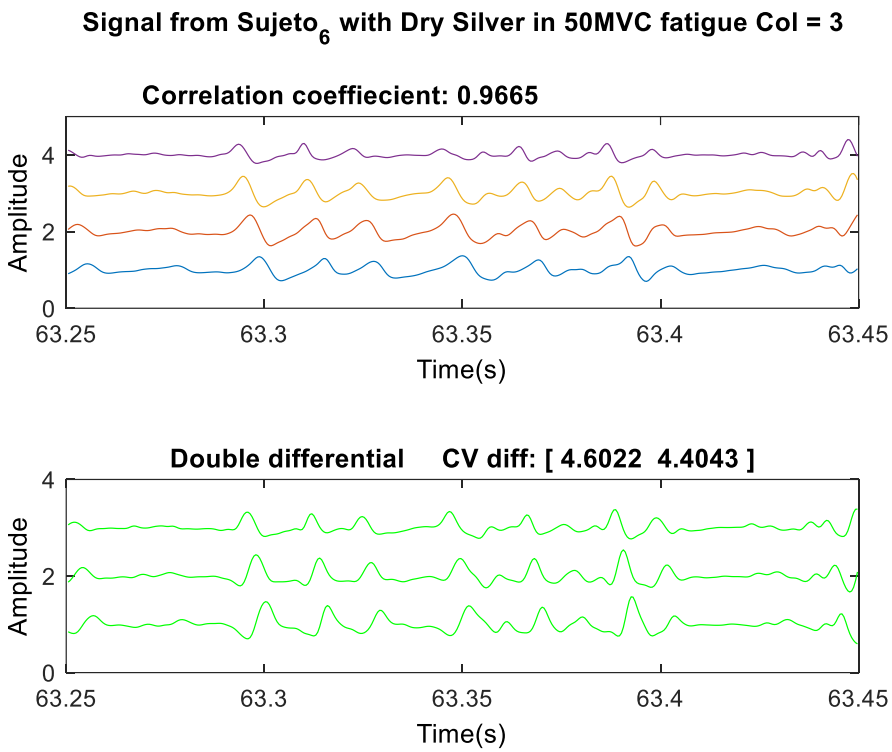

Figure 25: Time signal 2, Silver, 50% MVC

Material: Silver, 30% MVC

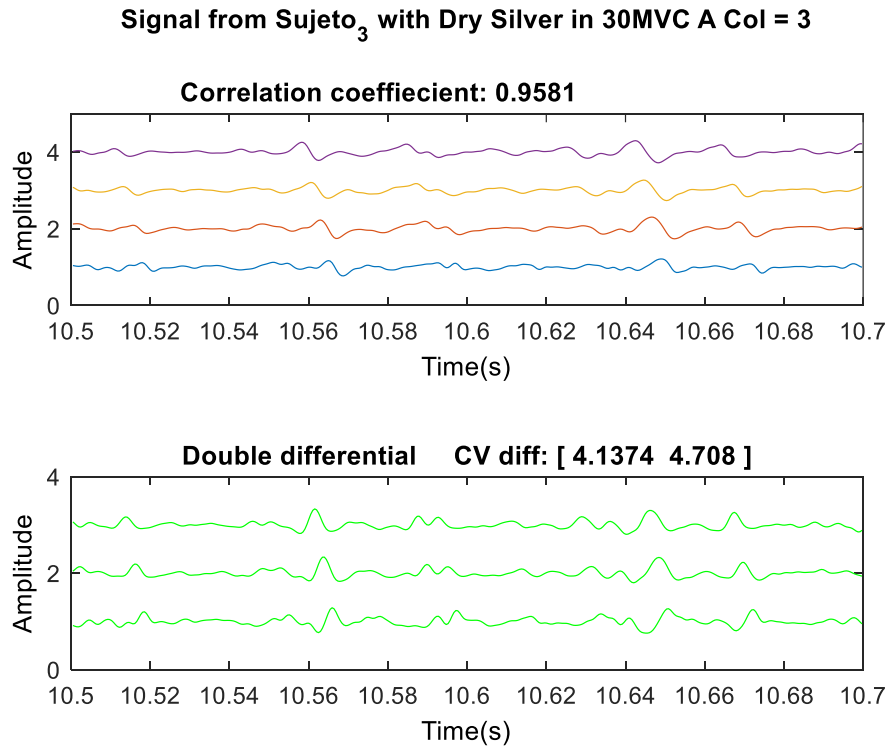

Figure 26: Time signal 3, Silver, 30% MVC

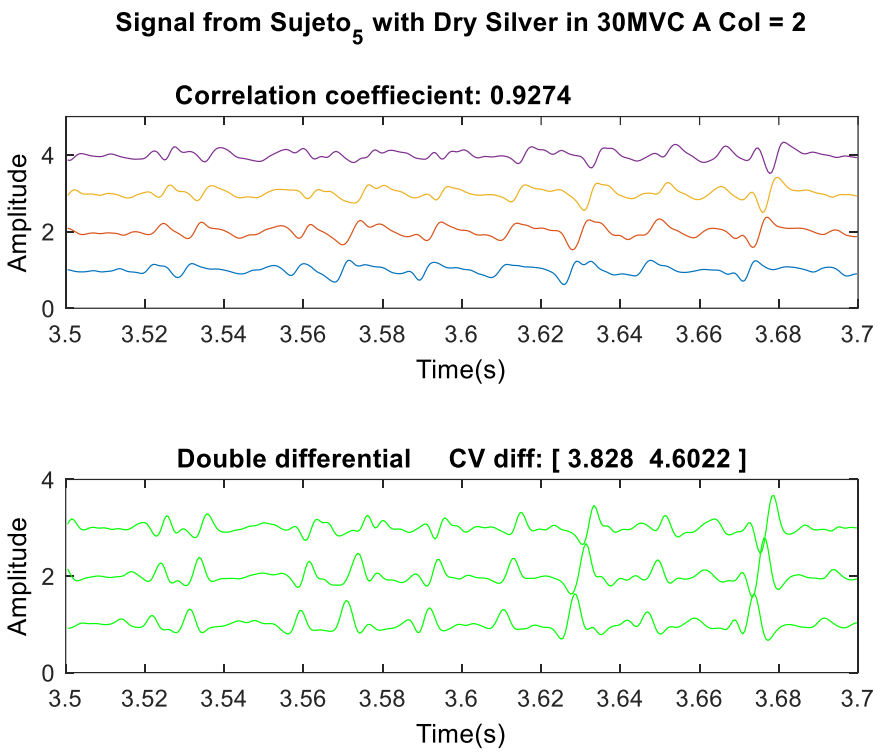

Figure 27: Time signal 4, Silver, 30% MVC

Material: Silver, 10% MVC

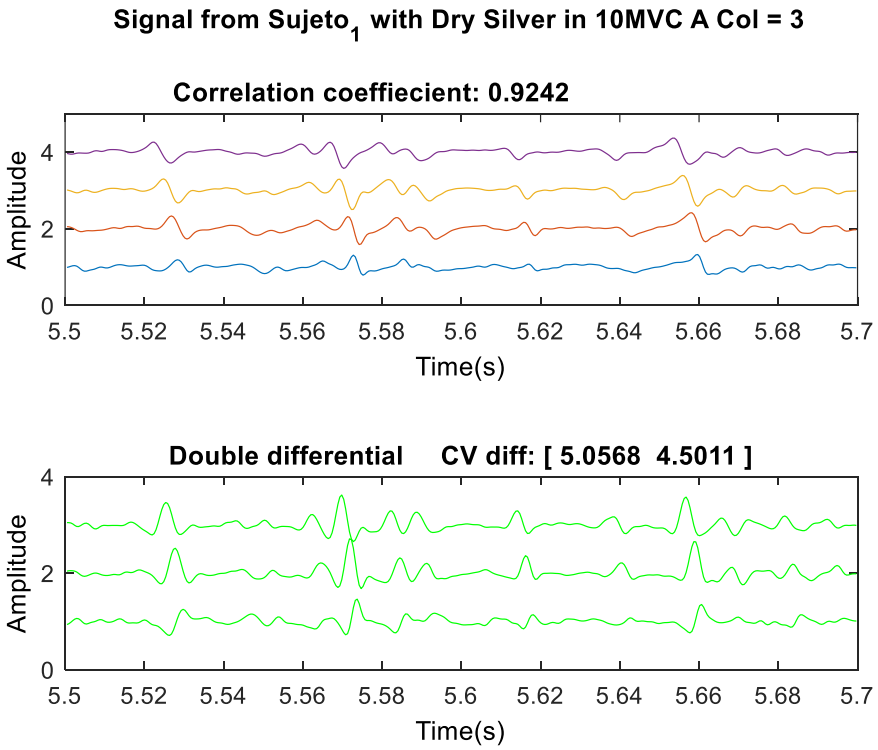

Figure 28: Time signal 5, Silver, 10% MVC

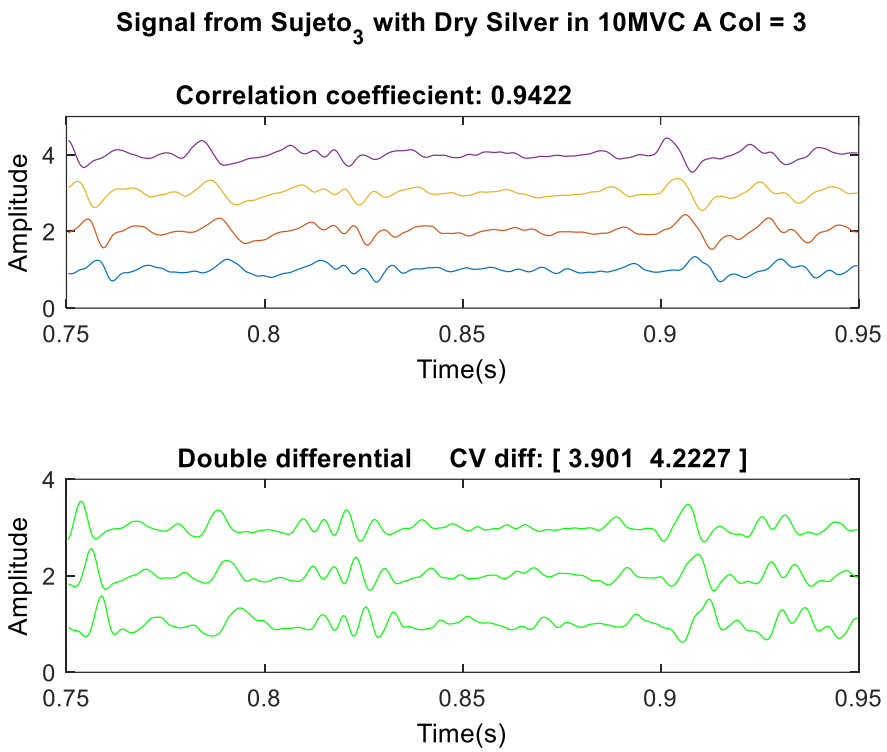

Figure 29: Time signal 6, Silver, 10% MVC

Material: Stainless steel, 50% MVC

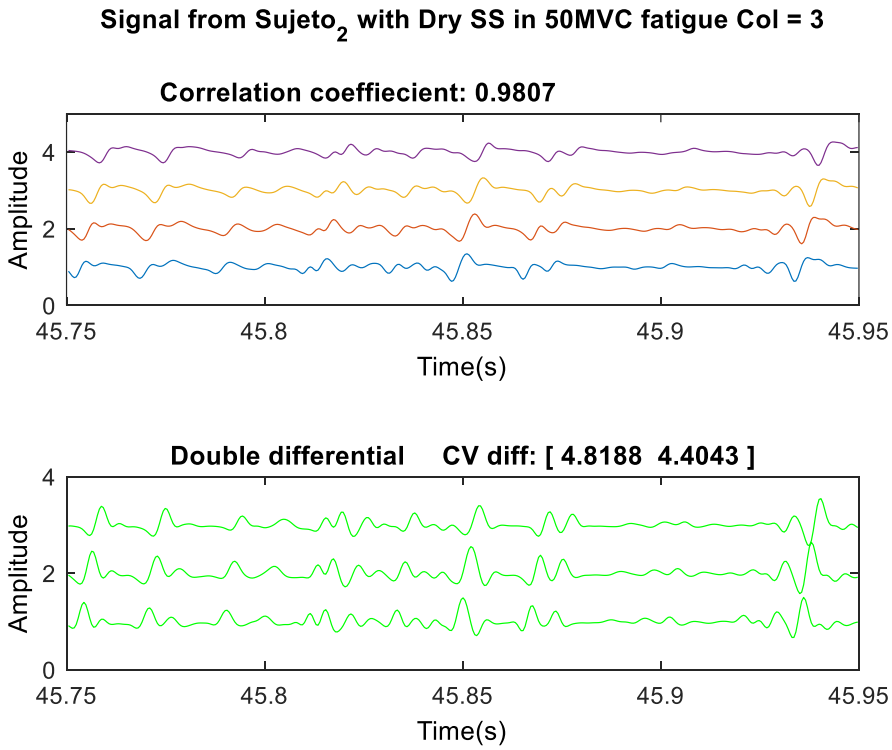

Figure 30: Time signal 7, Stainless steel, 50% MVC

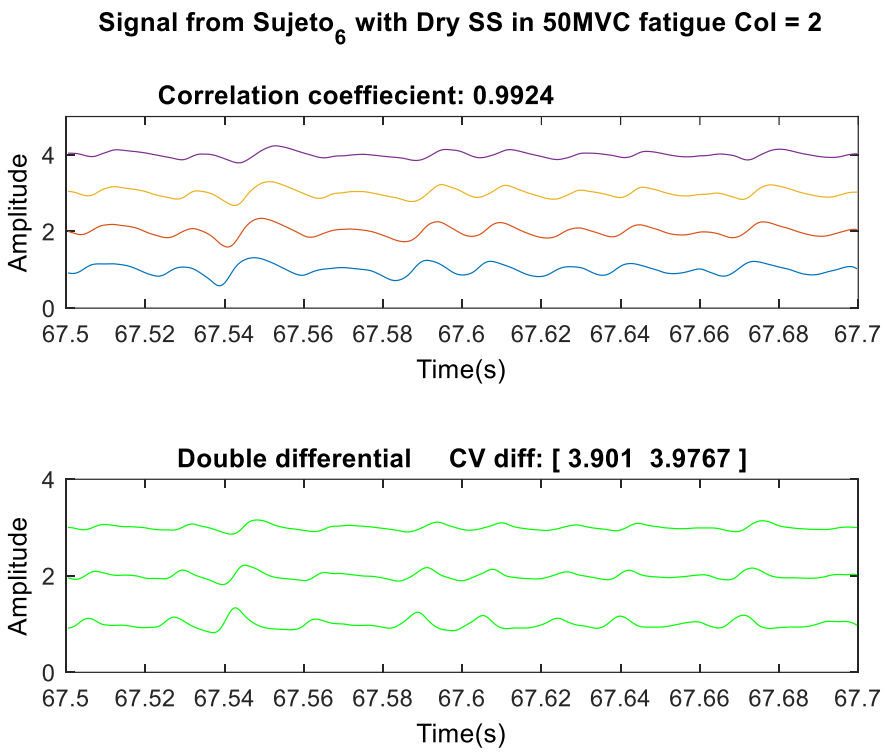

Figure 31: Time signal 8, Stainless steel, 50% MVC

Material: Stainless steel, 30% MVC

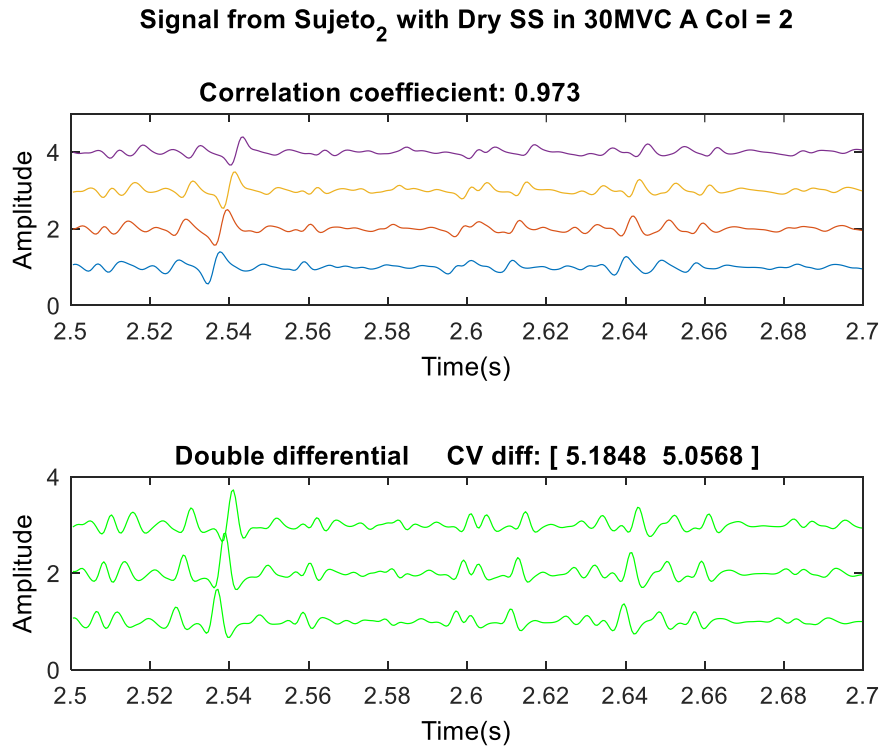

Figure 32: Time signal 9, Stainless steel, 30% MVC

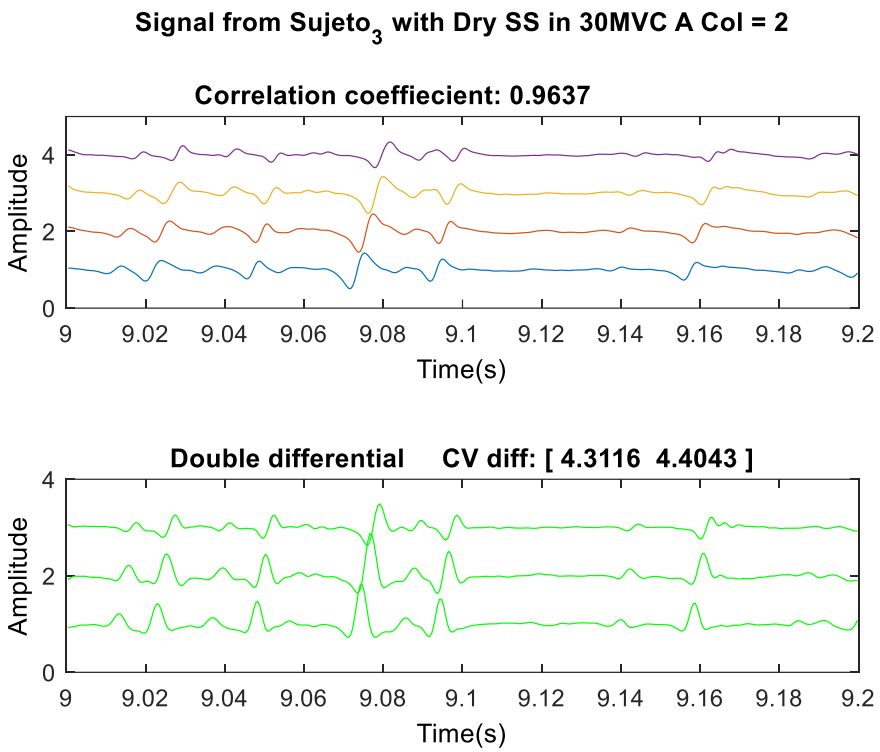

Figure 33: Time signal 10, Stainless steel, 30% MVC

Material: Stainless steel, 10% MVC

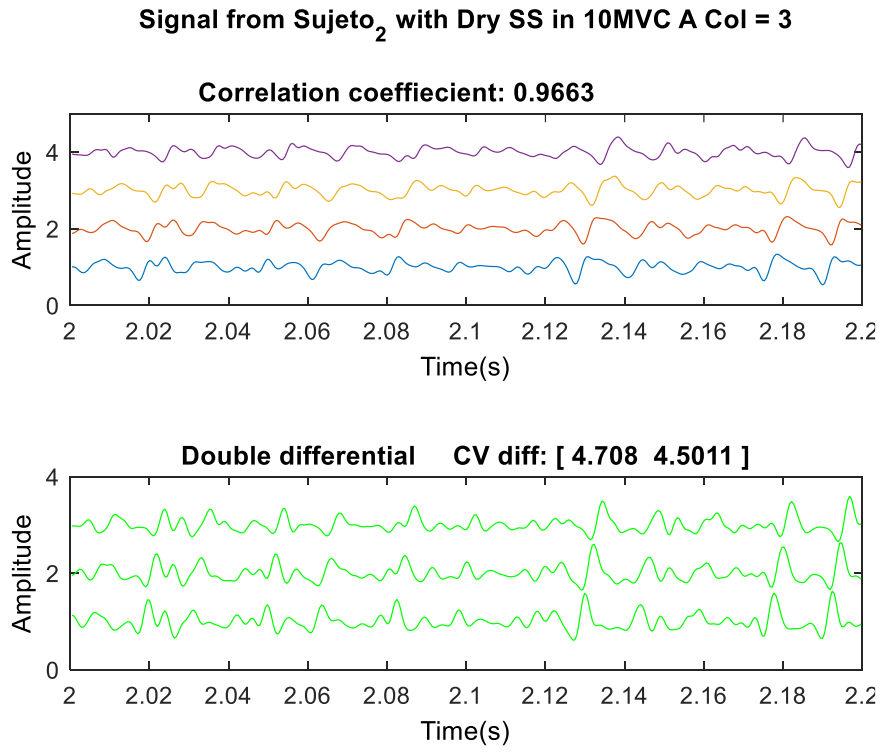

Figure 34: Time signal 11, Stainless steel, 10% MVC

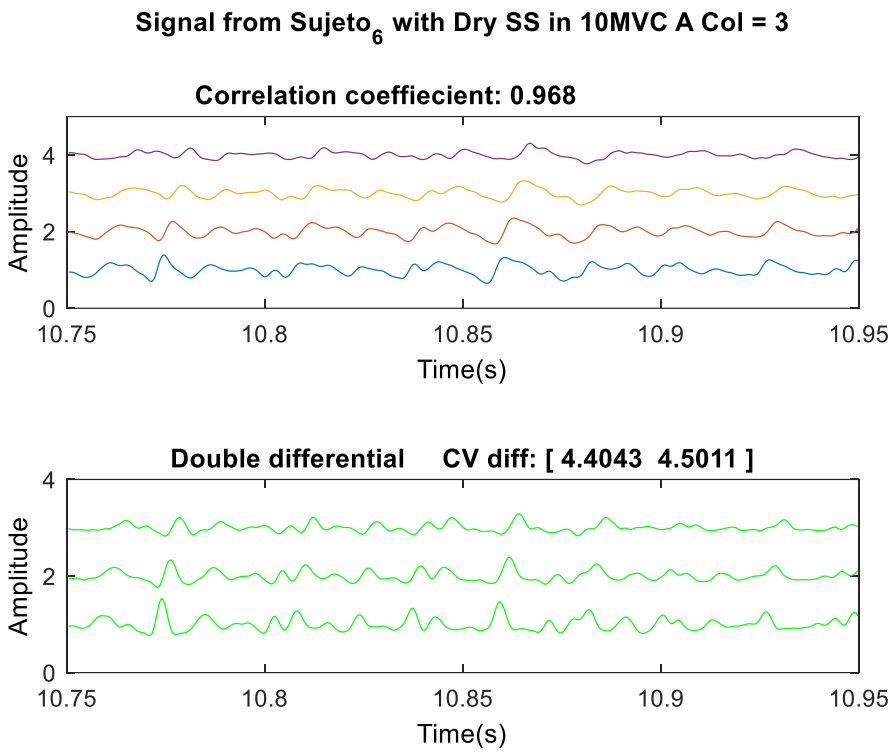

Figure 35: Time signal 12, Stainless steel, 10% MVC

4.1.2. Time series results

The results show in most cases clean signals both in single differential, SD, (upper window) and double differential, DD, (lower window), the motor unit action potential (MUAP) and its propagation along the channels can be visualized in silver and in stainless steel electrode arrays. The correlation coefficients, computed over the SD channels, are high and even though this could be the result of coupled noise in channels it can be noticed by visual inspection that noise does not have an impacting contribution in the signal quality.

The estimation of the conduction velocity, computed from the DD signals pairs, shows in almost all cases similar values, despite this result does not mean by itself a conclusive result (the estimation of the value could be wrong), it is a good result as the conduction velocities are expected to be similar in close areas (columns of the array) and the results acquired are inside the expected range.

4.2. Signal Spectra

The examples of both silver and stainless steel are depicted in each of the different MVC cases. In each graph the 16 single differential signals are represented in the frequency domain for a time segment of 500 ms. Although the sampling frequency was 2048 samples/second the resulting spectra has been cut to a 250 Hz bandwidth as little power was located in higher frequencies.

The method used to calculate the spectrum was Welch's method. This method splits the signal into sub segments that are windowed. The periodogram is calculated for each sub segment, afterwards the resulting periodograms are averaged to reduce the variance. As an example the 500 ms segment would be divided into smaller segments (sub segments) in each of this sub segments periodogram is calculated, then each of this periodograms are averaged keeping the signal spectral components (considered constant during along the sub segment) and reducing the variance.

4.2.1. Spectra graphs

Each channel spectrum is represented in a color in the graph.

50% MVC Spectrum

- Silver

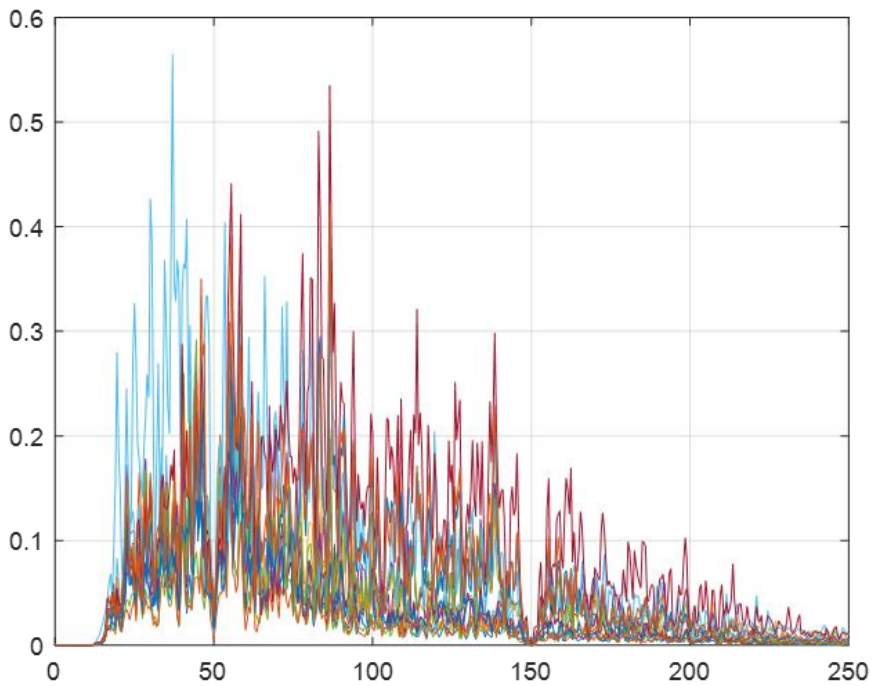

Figure 36: Spectrum Silver 50% MVC

- Stainless steel

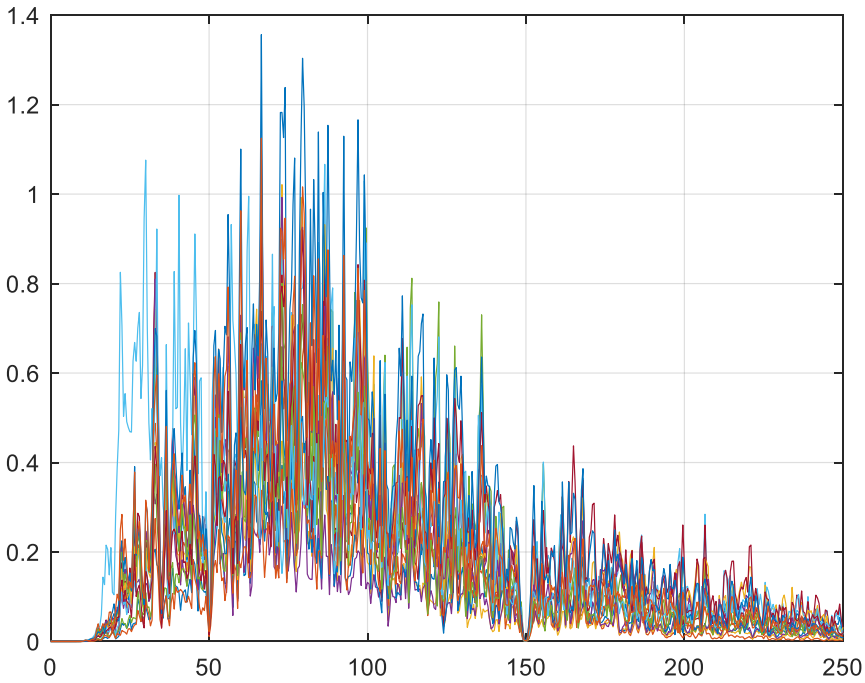

Figure 37: Spectrum Stainless steel 50% MVC

30% MVC Spectrum

- Silver

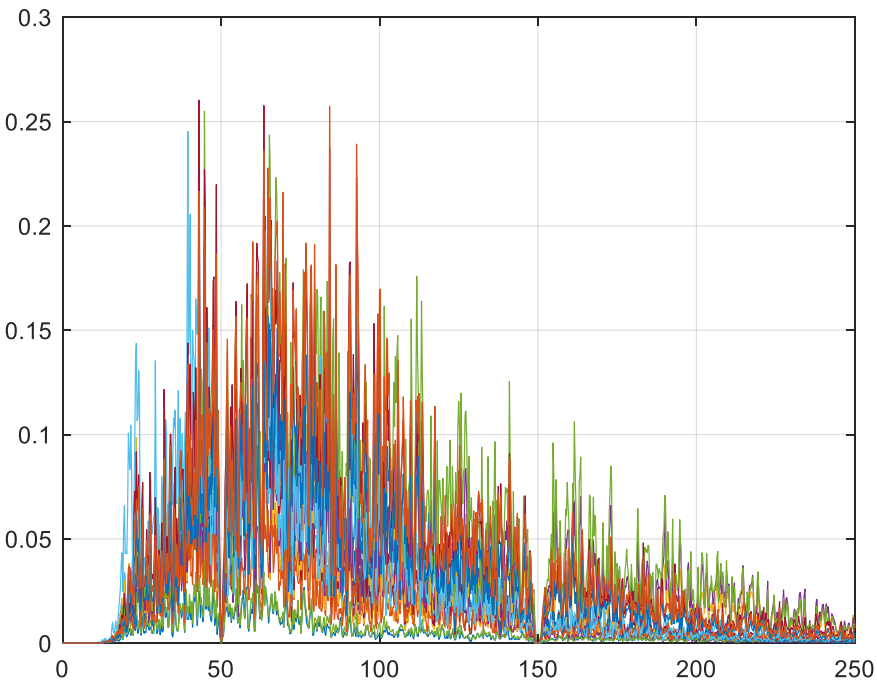

Figure 38: Spectrum Silver 30% MVC

- Stainless steel

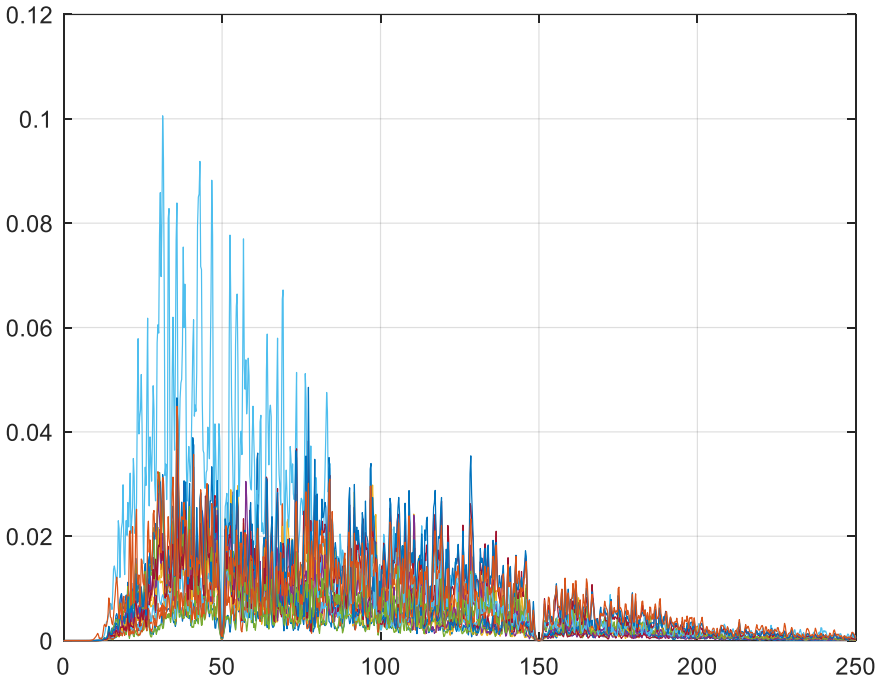

Figure 39: Spectrum Stainless steel 30% MVC

10% MVC Spectrum

- Silver

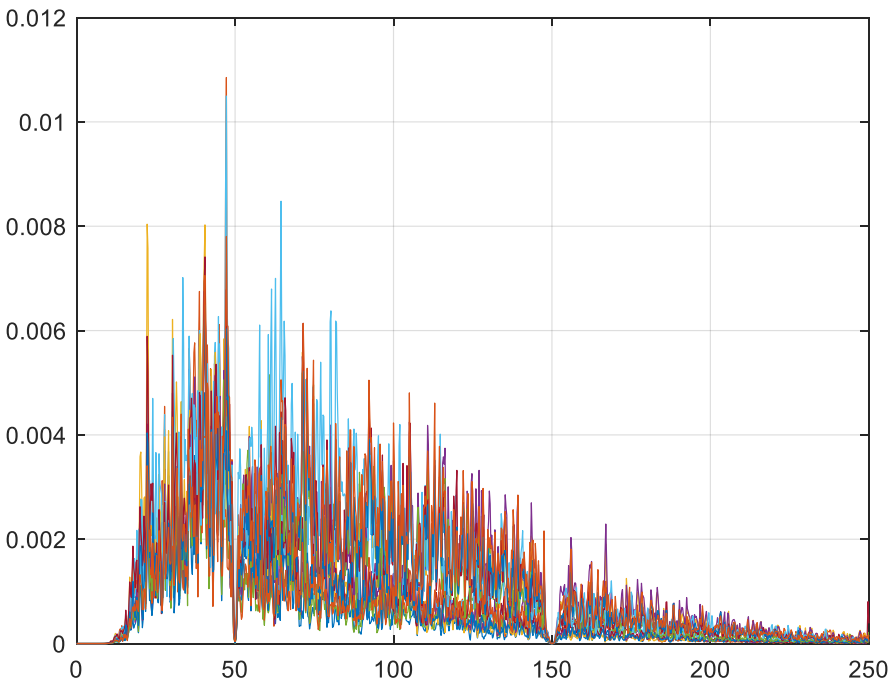

Figure 40: Spectrum Silver 10% MVC

- Stainless steel

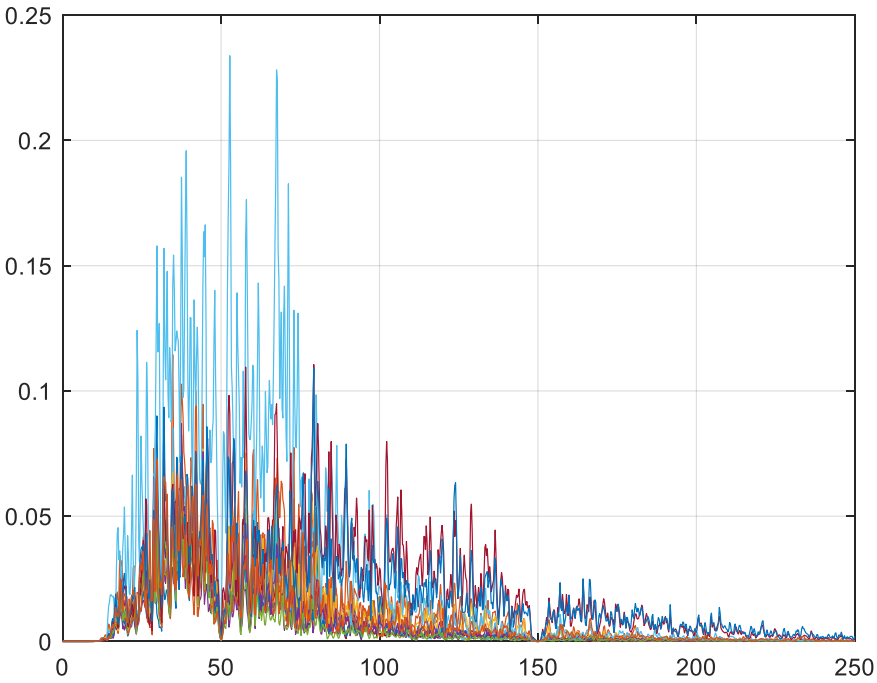

Figure 41: Spectrum Stainless steel 10% MVC

4.2.2. Spectra graphs, separate channels

In this section the four first channels of each array have been plotted separately in order to observe better the shapes of some of them in each situation. The plots are from different subjects in respect the previous section.

50% MVC Spectrum

- Silver

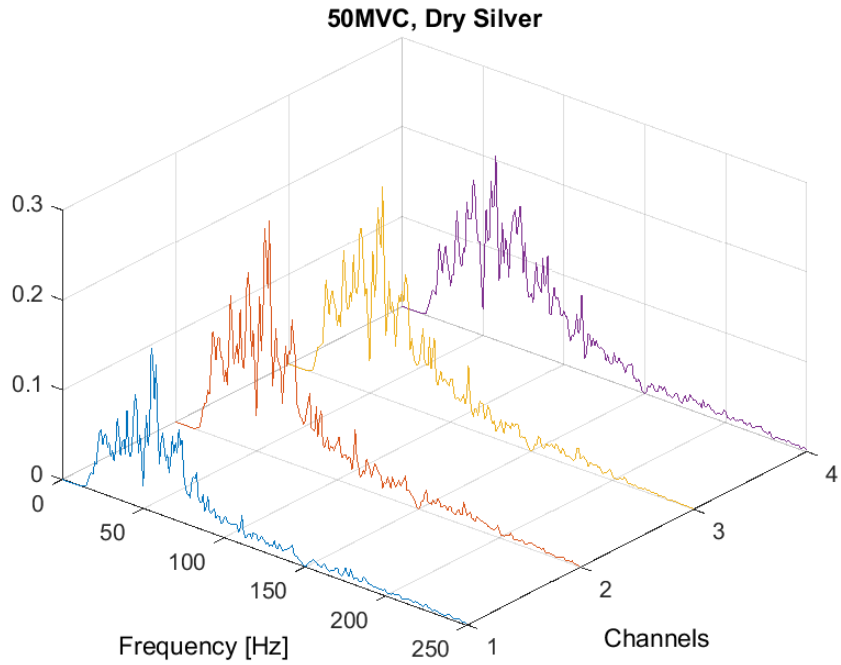

- Stainless steel

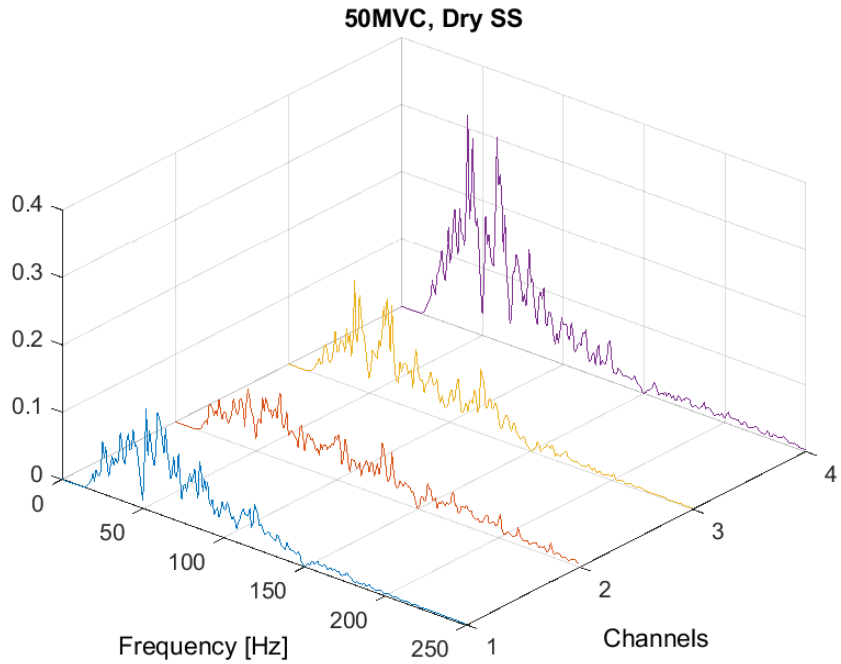

30% MVC Spectrum

- Silver

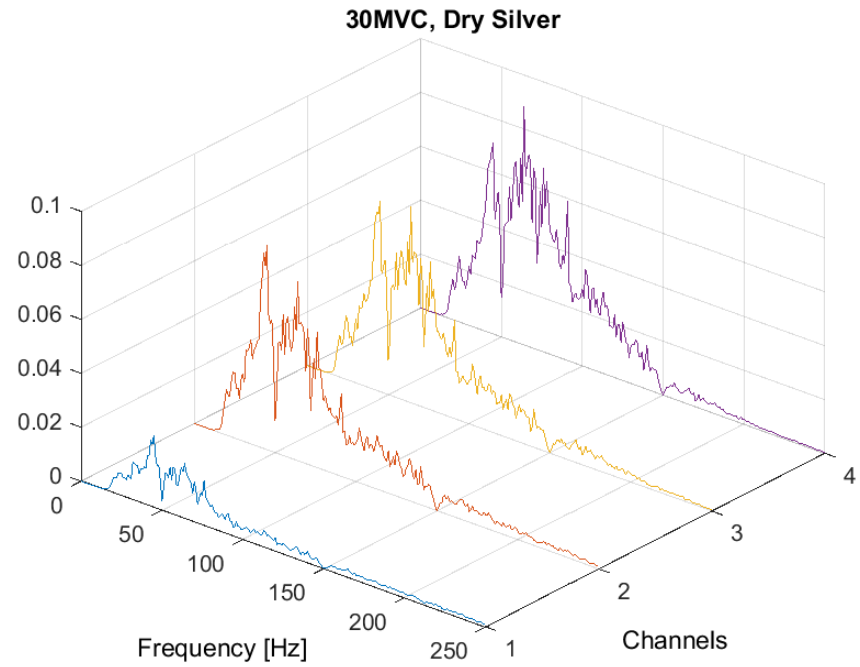

- Stainless steel

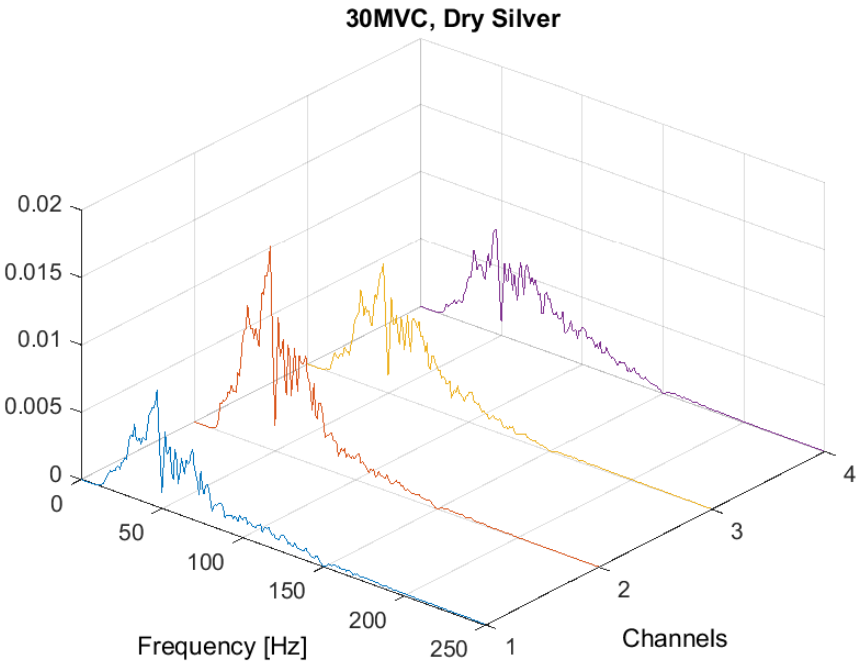

10% MVC Spectrum

- Silver

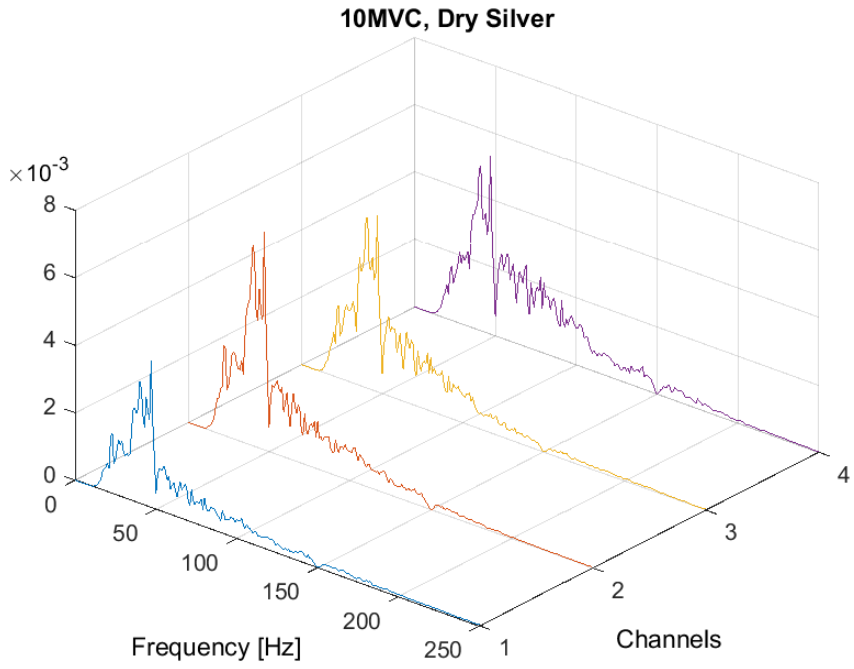

- Stainless steel

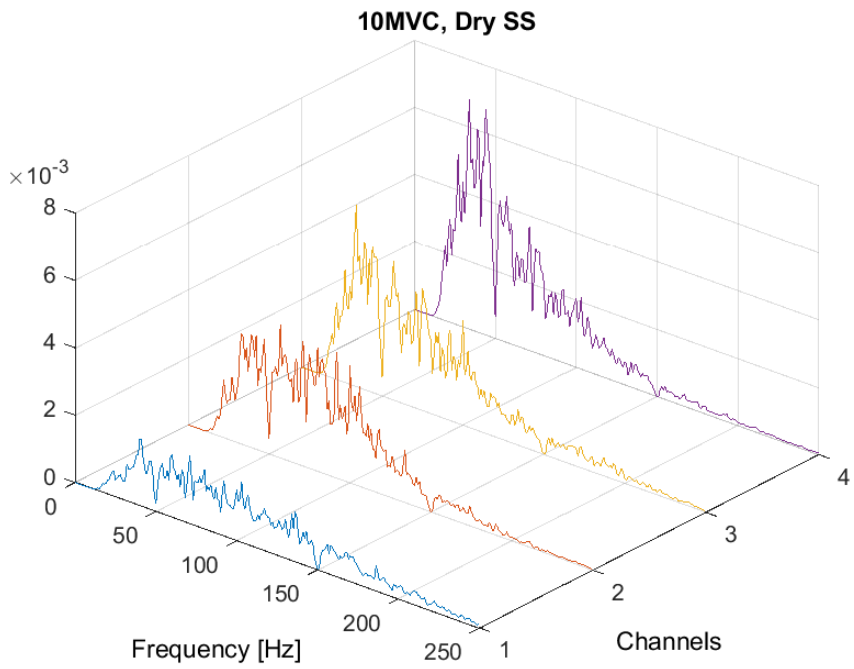

4.2.3. Signal spectra results

The results of the spectra analysis show an expected power distribution along the frequencies. A big part of the total power is concentrated at lower frequencies. The effect of the notch filters is clearly visualized surrounding 50 and 150 Hz.

4.3. Bivariate analysis

In the following section, the variables of conduction velocity CV and the correlation coefficient of the time segments are analyzed at the same time. This analysis is performed in order to separate segments and detect how many of them deliver valid information.

To select what is valid information referring the CV computed in a segment it is necessary at least to have a high correlation coefficient 0.8 and the CV to be inside a human feasible range from 3 to 6 m/s.

The first attempt to represent the samples (segments) was using a scatterplot shown in the following image. There are six colors representing the three initial arrays in both situations with gel and without gel (dry).

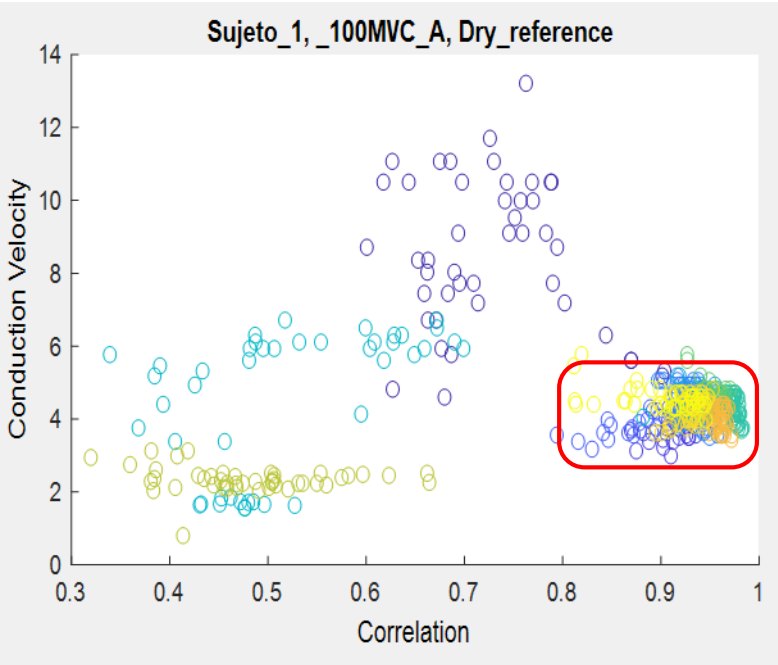

Figure 42: Scatter plot showing Correlation coefficient and CV

The main problem with this approach is the difficulty to properly visualize and quantify the amount of samples inside the region defined. To solve this, a bivariate analysis in the form of 2-D histogram was used. This way it was easier to separate regions. In the following image, a red circled area shows approximately the region with valid samples.

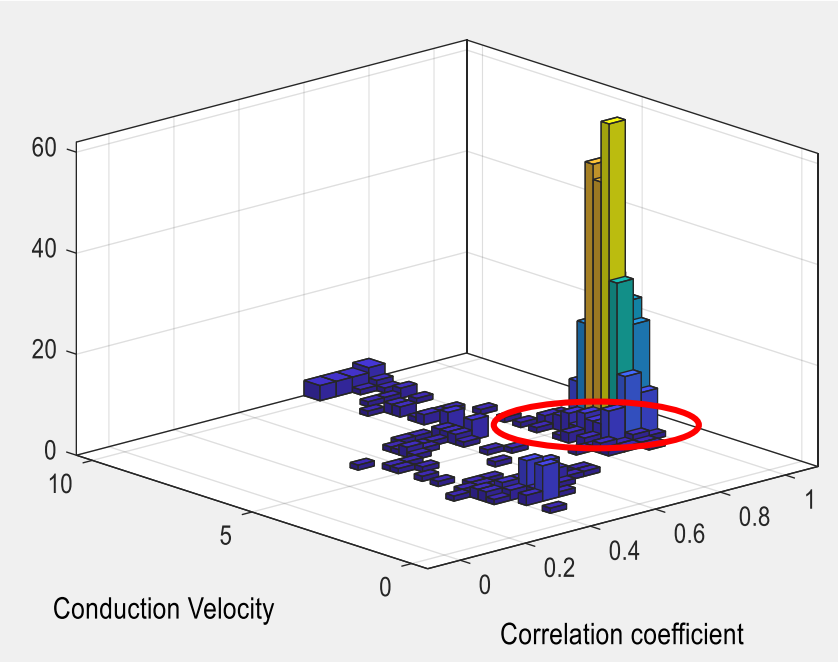

Figure 43: Bivariate graph Correlation coefficient /CV

Following this approach, four cases are represented, both materials, silver and stainless steel, with both single differential signals and double differential signals. In each case the representation of the four MVC acquisitions are included.

4.3.1. Bivariate analysis graphs

Material: Silver, single differential

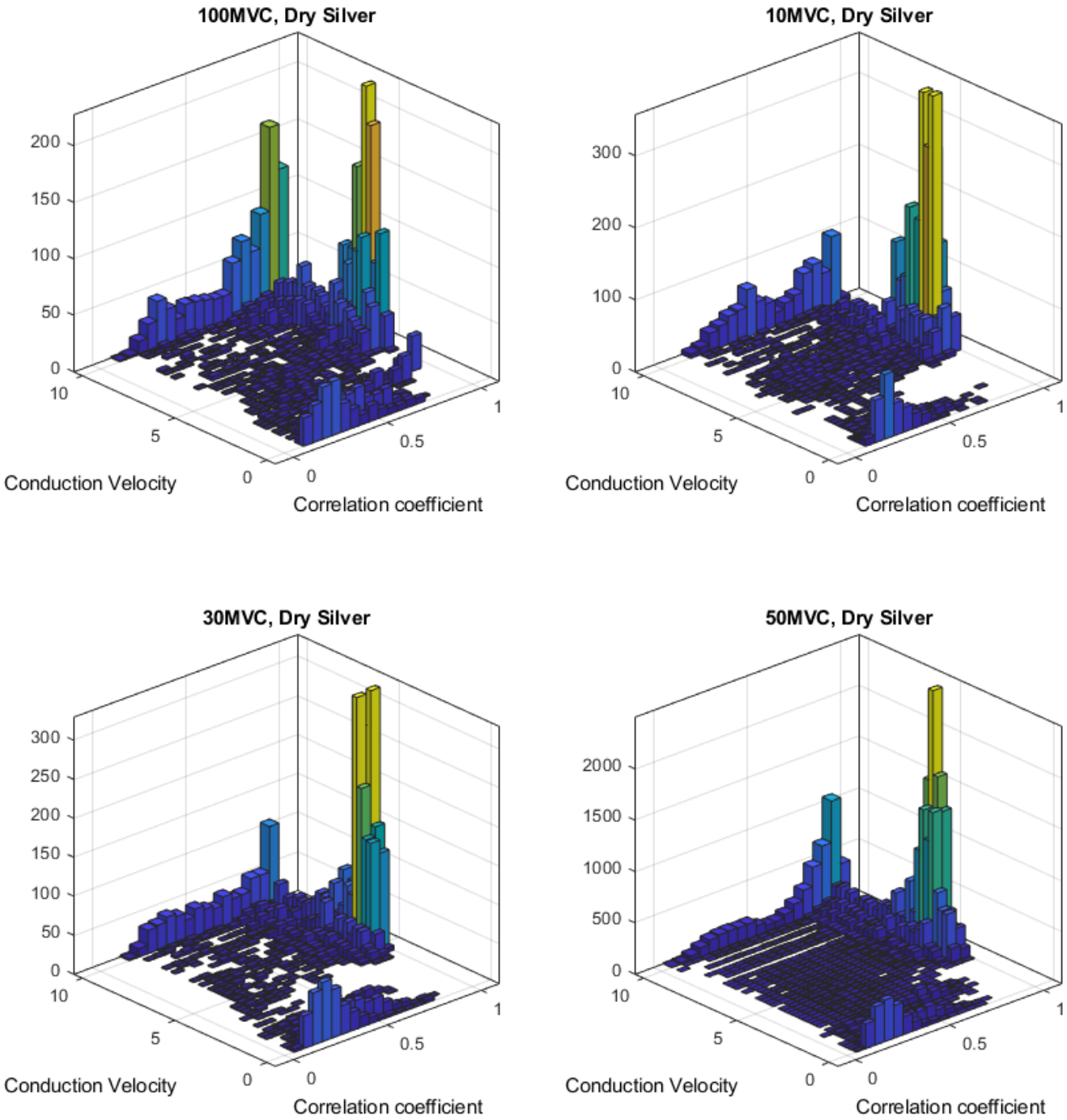

Figure 44: Bivariate analysis Silver SD

Material: Silver, double differential

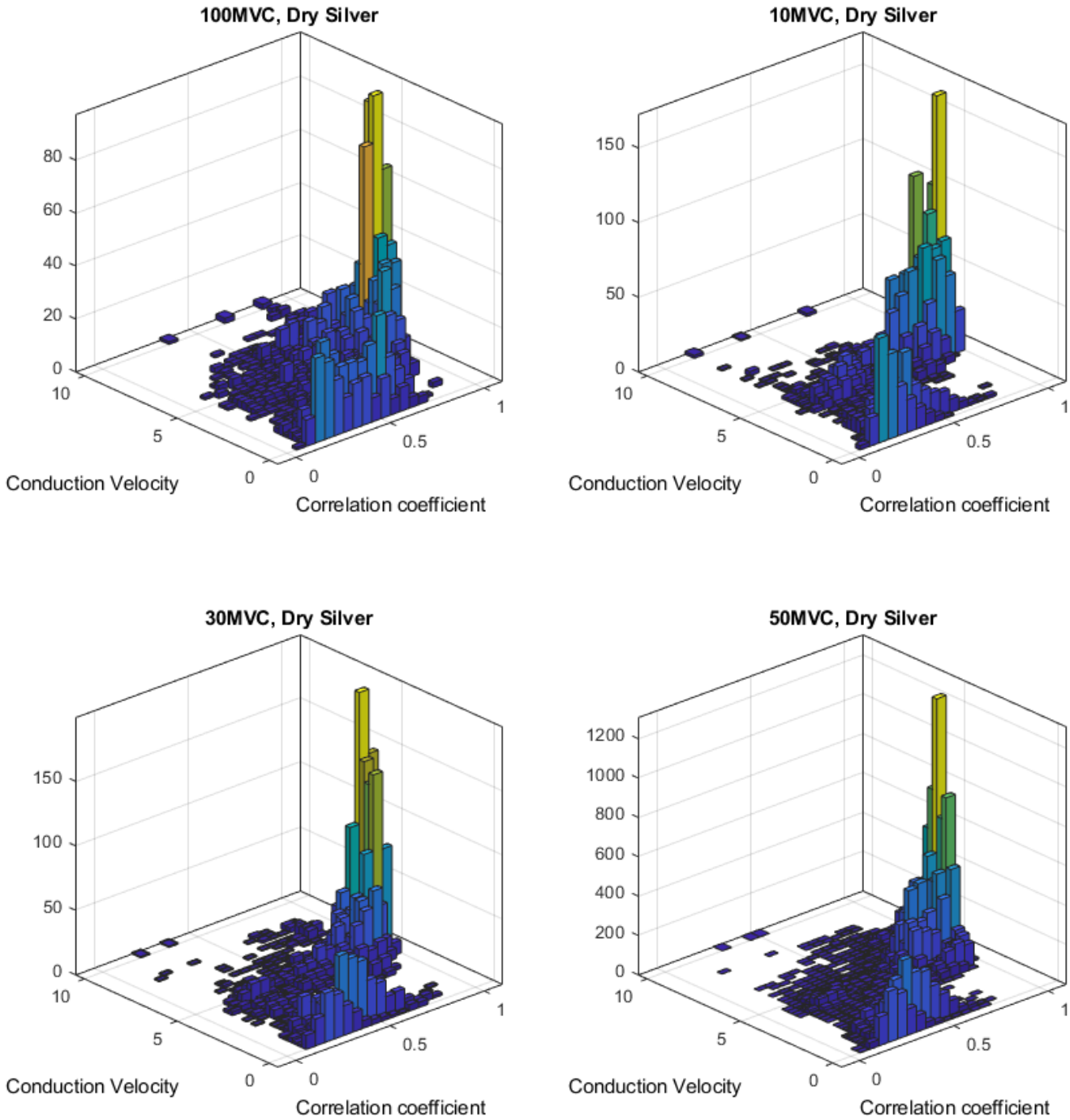

Figure 45: Bivariate analysis Silver DD

Material: Stainless steel, single differential

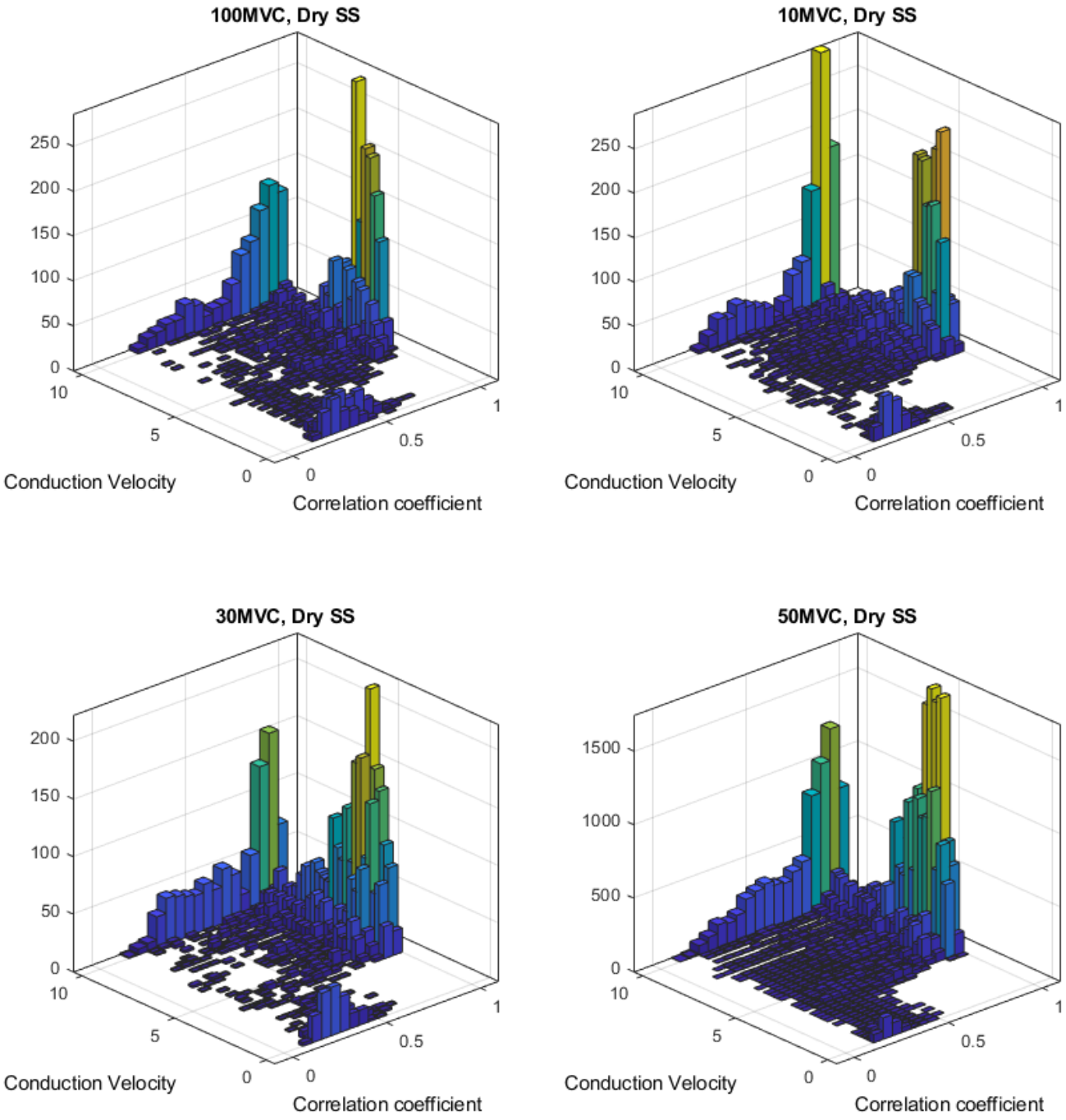

Figure 46: Bivariate analysis Stainless steel SD

Material: Stainless steel, double differential

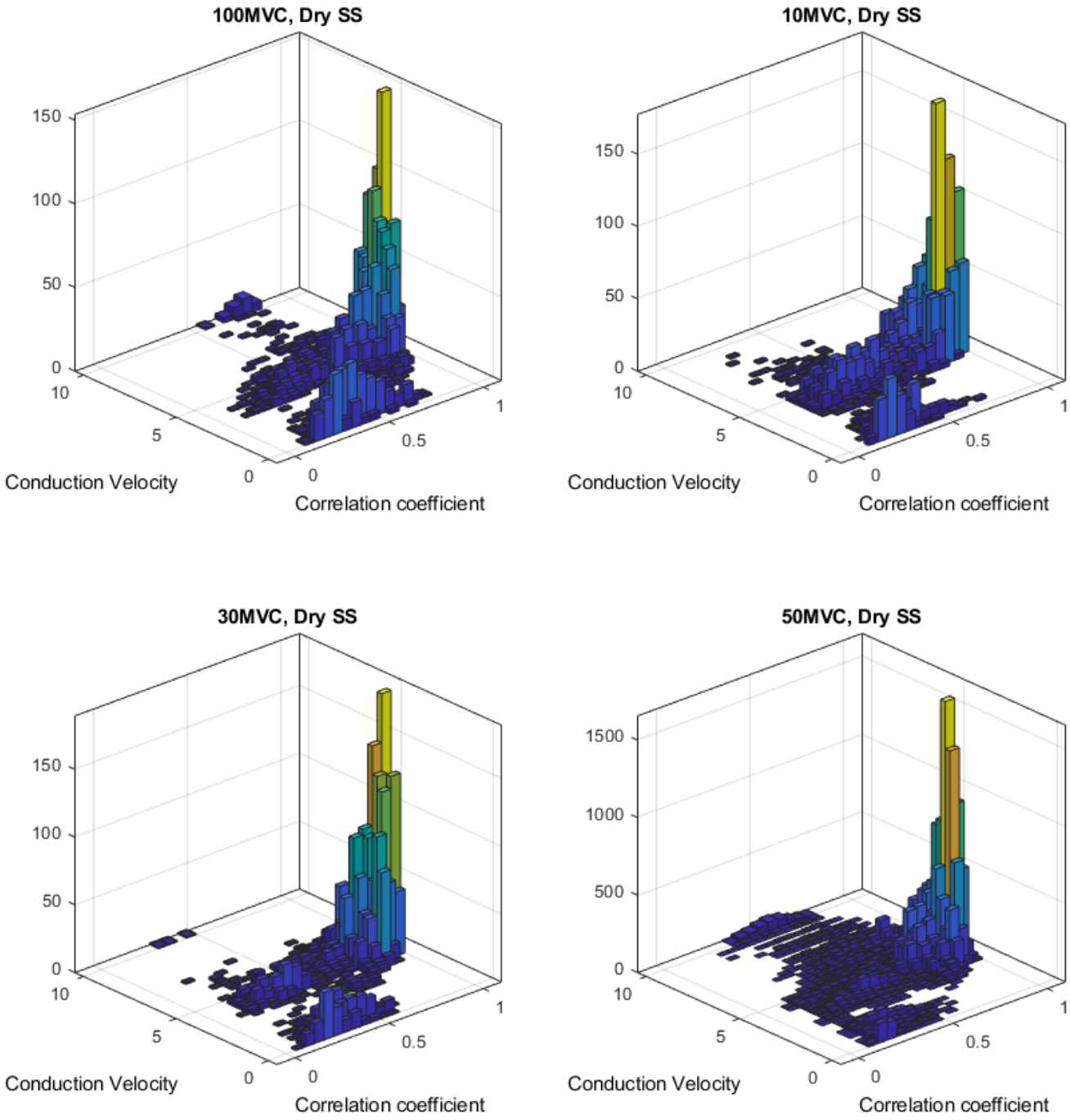

Figure 47: Bivariate analysis Stainless steel DD

4.3.2. Bivariate analysis results

First of all, and focusing first on single differential bivariate analysis, it can be observed that a lot of samples fall in regions out of the expected human range of CV (all values above 10 m/s are represented in the section just above that level in the graphics). Although a lot of values are concentrated in the area with high correlation (close to 1 in the correlation axis perspective) there are still spread samples both low correlation zones and zones out of the CV human range.

As explained in the times series results, the values with high correlation and an out of range CV (much higher) may be caused by some channels with coupled noise from the power line for example. This perturbation can reach the array and the channels at a much higher speeds than the EMG signal having therefore a very little delays between very correlated channels, what gives high correlation coefficients and big, out of range, CV. Another possibility could be movement artifacts as they would affect the array almost at the same time but since the contraction of the muscle is sustained and the exercise is isometric this possibility should not have a high impact.

On the other hand, the results in double differential bivariate analysis show a better performance compared to SD, the double differentiation reduces the effect of non-traveling potentials, noises that affect all the electrodes at the same time like the one coming from the power line. In this case, most of the samples out of human range have disappeared and even though there are still some samples with low correlation most of the samples are in the meaningful area having correlations higher than 0.8 and in CV human range.

At the first view comparing double differential signals of silver and stainless steel the performance seems comparable as the improvements and the areas where the samples are concentrated are the expected ones, however taking a closer look it can be observed that stainless steel has less samples with low correlation and more samples concentrated in the meaningful area, specially the 50 MVC exercise that, as it has duration of two minutes, has more samples depicted and the graph that corresponds to stainless steel show very few samples with low correlation coefficient.

4.4. Intensity analysis

In this section the RMS value of the signals in the different arrays and exercises is evaluated (Rojas-Martínez, Mañanas, and Alonso 2012), the channels have been averaged. In these cases the graph shows both materials silver and stainless steel besides an extra array named afterwards as “reference” although is just the silver array from the BIOART group (Figure 15is depicted with the same exercises performed in the subject with gel and dry approach. The representation form is a boxplot, a descriptive statistical graph that helps to summarize.

4.4.1. Intensity analysis graphs

The y-axis shows RMS value, in the x-axis there are two indexes first one represents the array being 1 - Dry reference, 2 - Gel reference, 3 - Silver, 4 - Stainless steel, and the second one the exercise number being, 2 – 10% MVC, 3 – 30% MVC, 4 – 50% MVC.

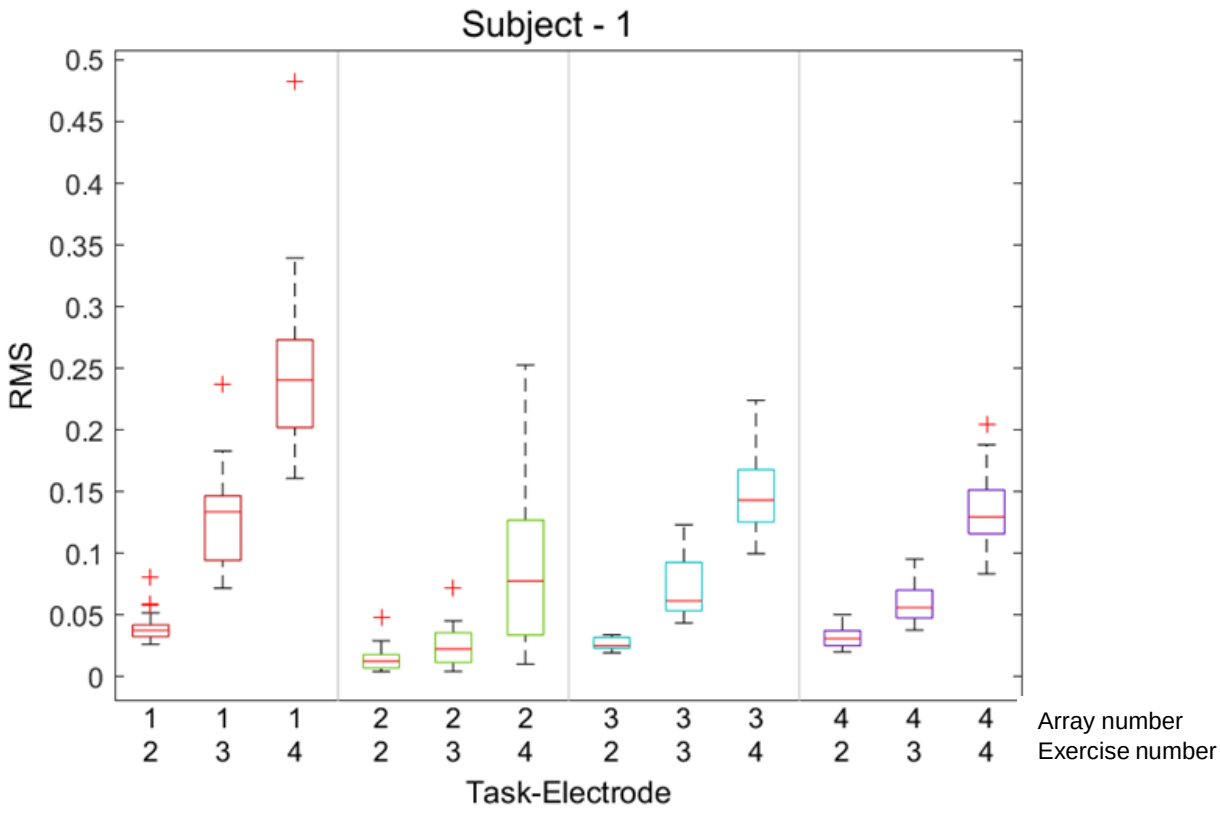

Figure 48: Intensity analysis, Boxplot 1

Array number:	1 - Dry reference 2 - Gel reference 3 - Silver 4 - Stainless steel

Exercise number:	2 - 10% MVC 3 - 30% MVC 4 - 50% MVC

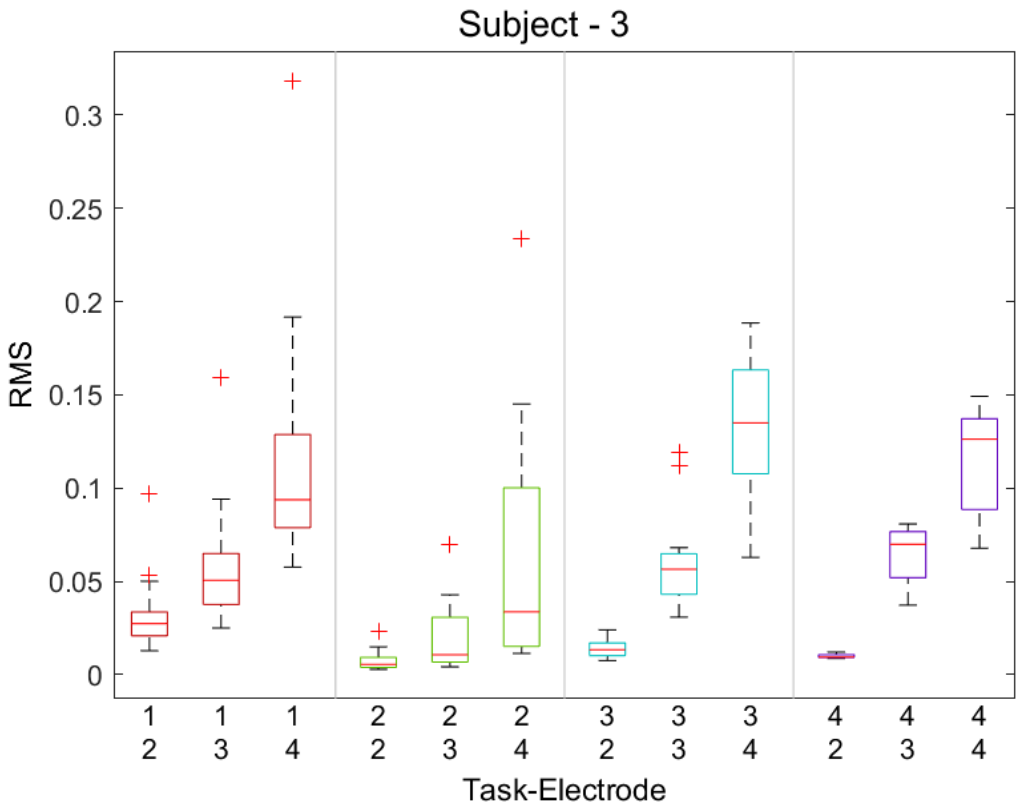

Figure 49: Intensity analysis, Boxplot 2

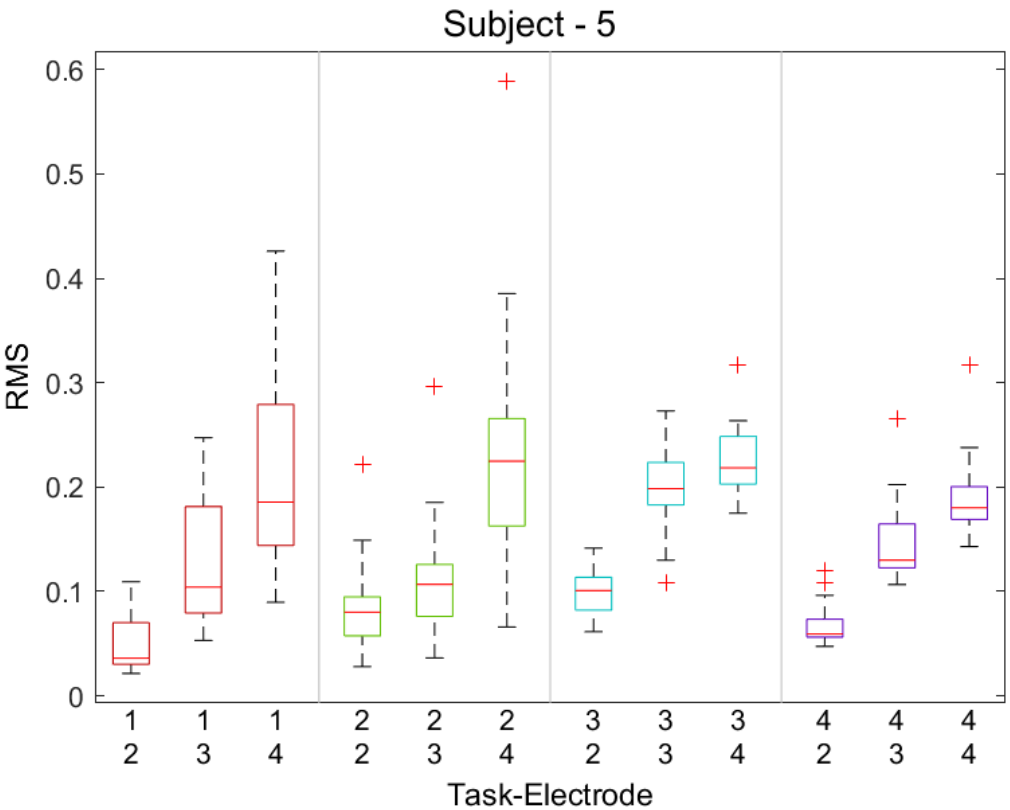

Figure 50: Intensity analysis, Boxplot 3

For the last graph all the subject's values have been averaged.

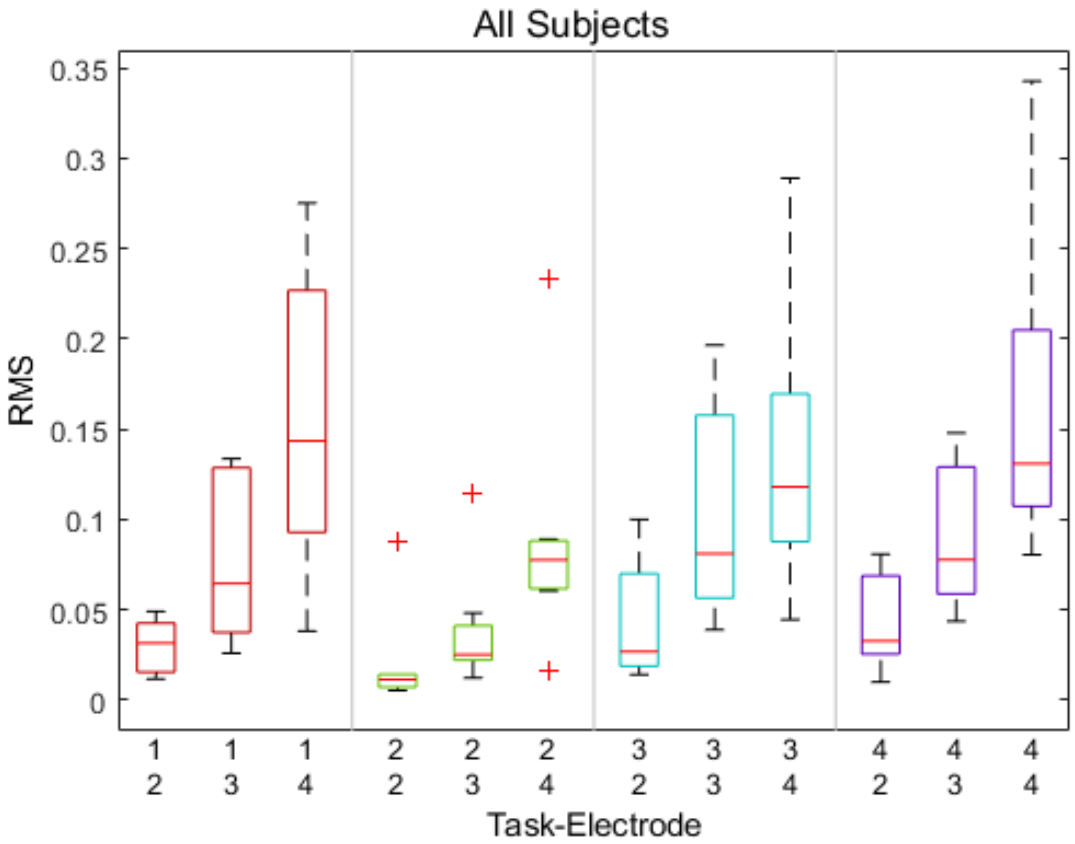

Figure 51: Intensity analysis, Boxplot 4, all subjects

4.4.2. Intensity analysis results

In the columns 1 and 2 the results of the array from BIOART with dry and gel applied situations show a big variance in the first case with RMS levels similar to the other two arrays and in the second case less variance but lower RMS levels.

Focusing on the columns 3 and 4, silver and stainless steel respectively, the results show comparable RMS values for both materials. In the las graph, that averages the results of all the subjects the medians of the three exercises are almost aligned and the quartiles are not very different one from the other showing a similar behaviour of the materials.

4.5. Boxplots of Conduction Velocity (CV)

In this part, the boxplot is used to represent the CV of the arrays already mentioned in the intensity analysis (Figure 15: Silver array from BIOART) so four array cases then both single differential and double differential and for each of the four exercises.

In order to represent valid data in the boxplots, only the samples (segments) with a correlation coefficient higher than 0.8 have been taken into account. In the y-axis is shown the percentage of the total number of samples that accomplish this criteria, in some cases columns are missing. This is because none of the samples in that subject reached the minimum of 0.8.

4.5.1. Boxplots of Conduction Velocity graphs

Exercise 1: 100% MVC, Single differential

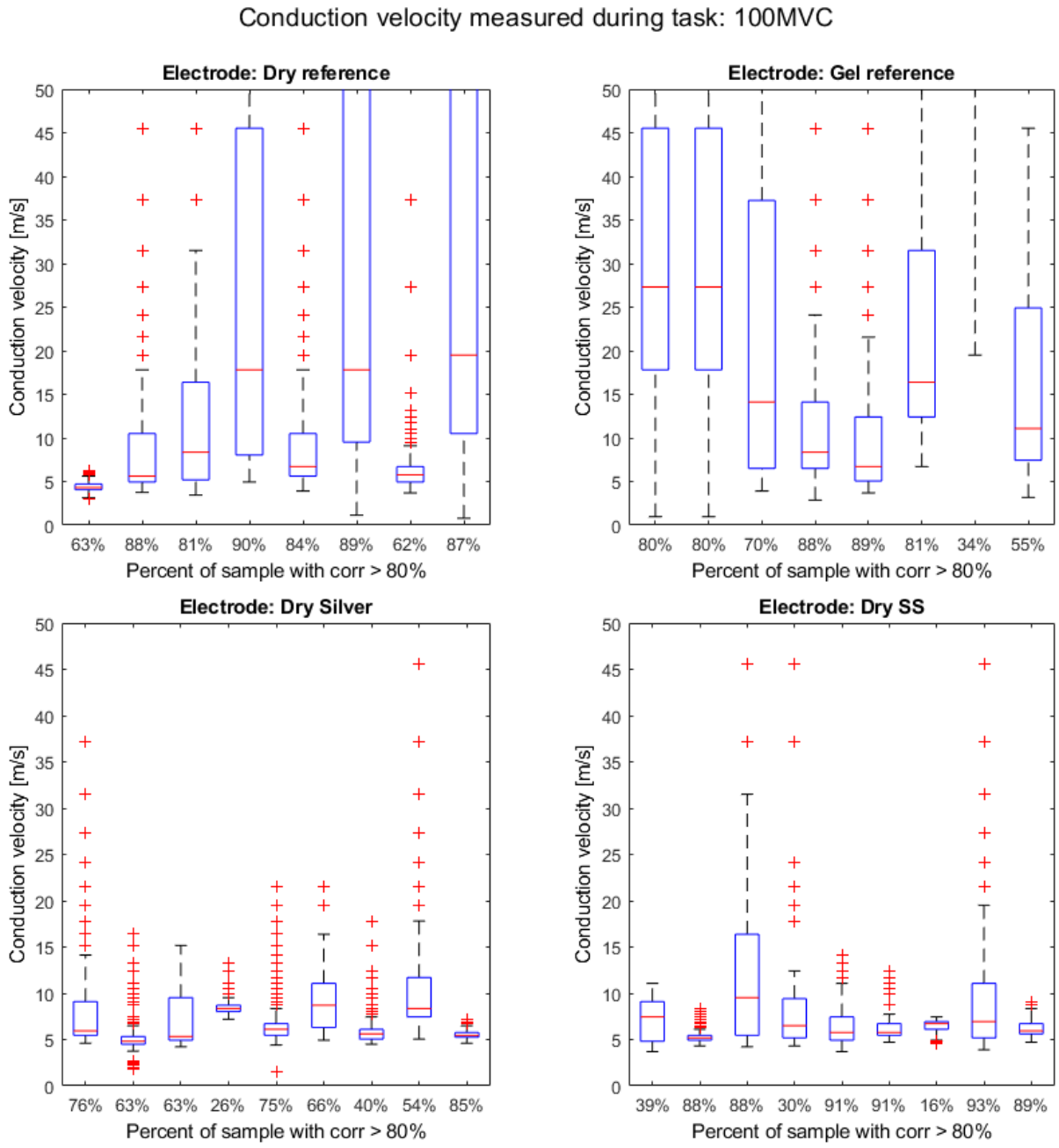

Figure 52: Conduction Velocity boxplot 100% MVC SD

Exercise 1: 100% MVC, Double differential

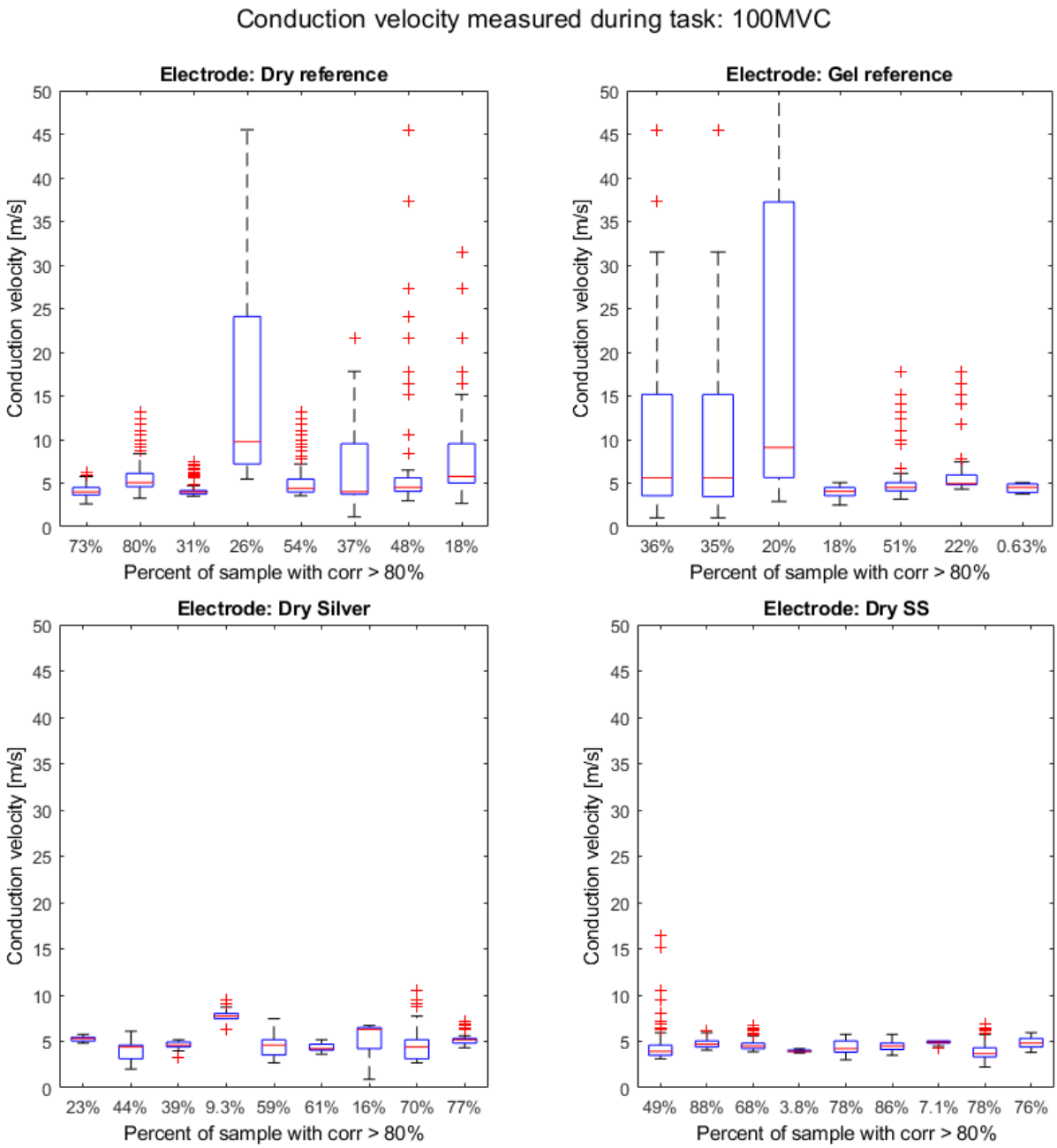

Figure 53: Conduction Velocity boxplot 100% MVC DD

Exercise 2: 10% MVC, Single differential

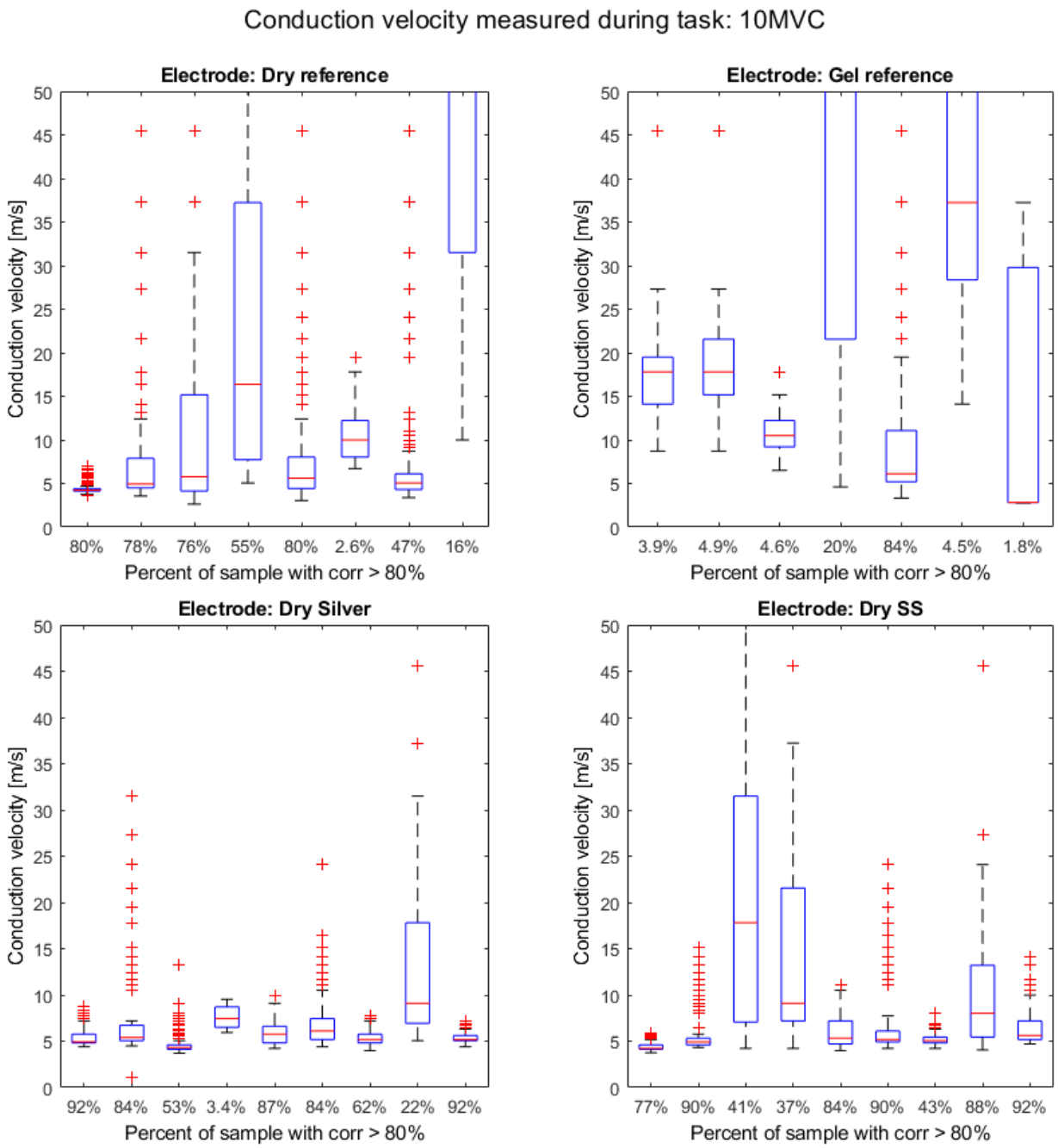

Figure 54: Conduction Velocity boxplot 10% MVC SD

Exercise 2: 10% MVC, Double differential

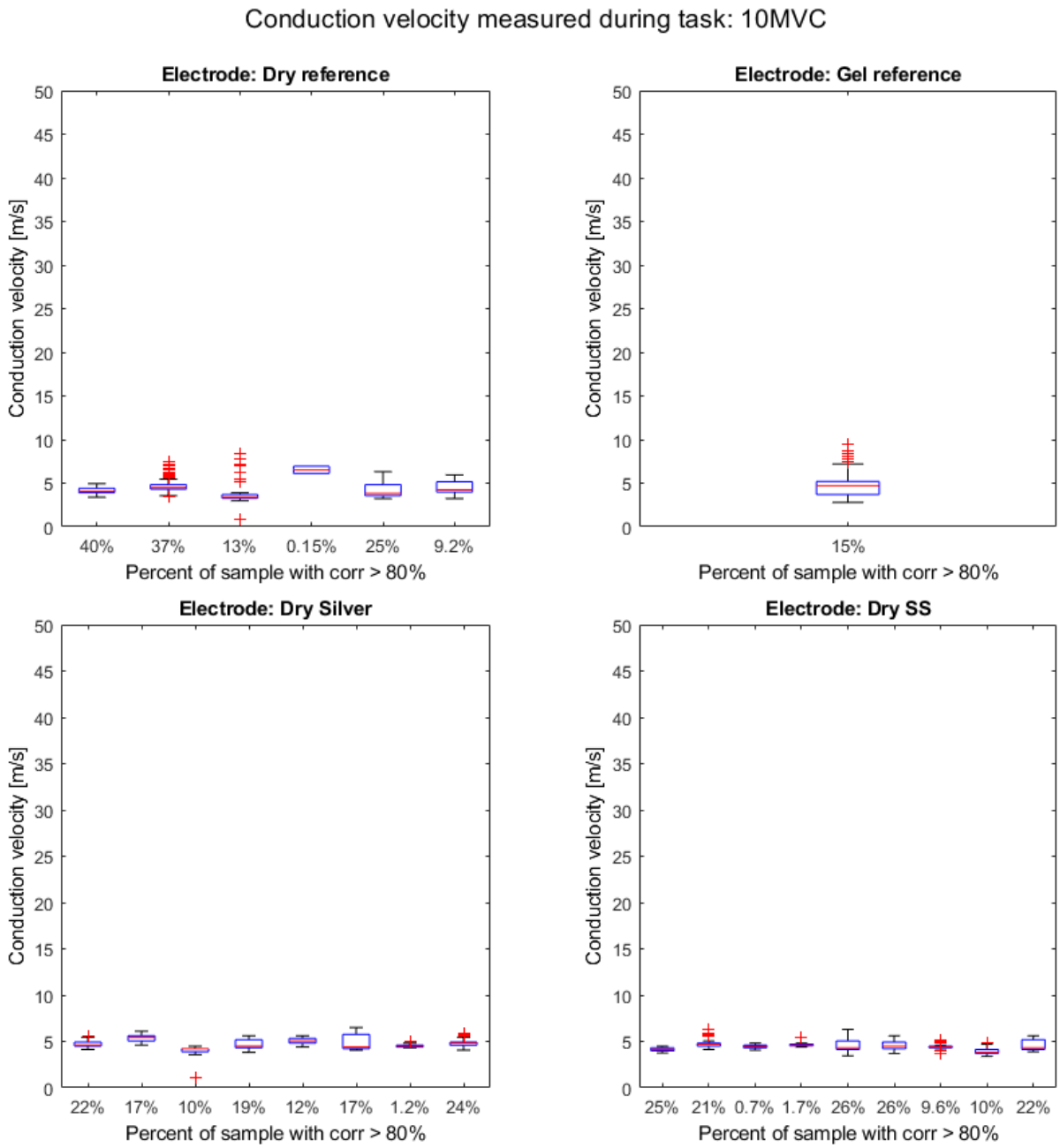

Figure 55: Conduction Velocity boxplot 10% MVC DD

Exercise 3: 30% MVC, Single differential

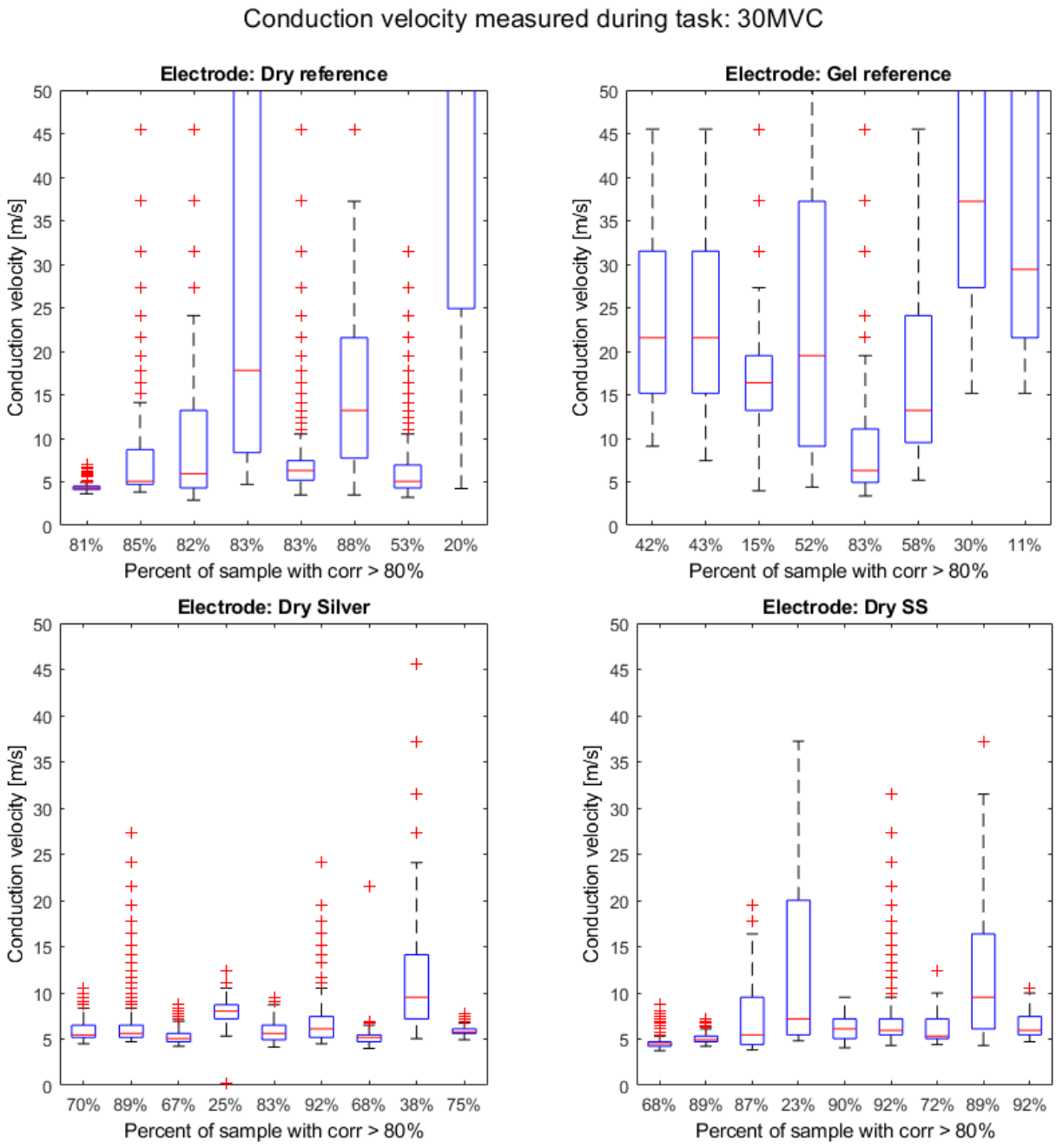

Figure 56: Conduction Velocity boxplot 30% MVC SD

Exercise 3: 30% MVC, Double differential

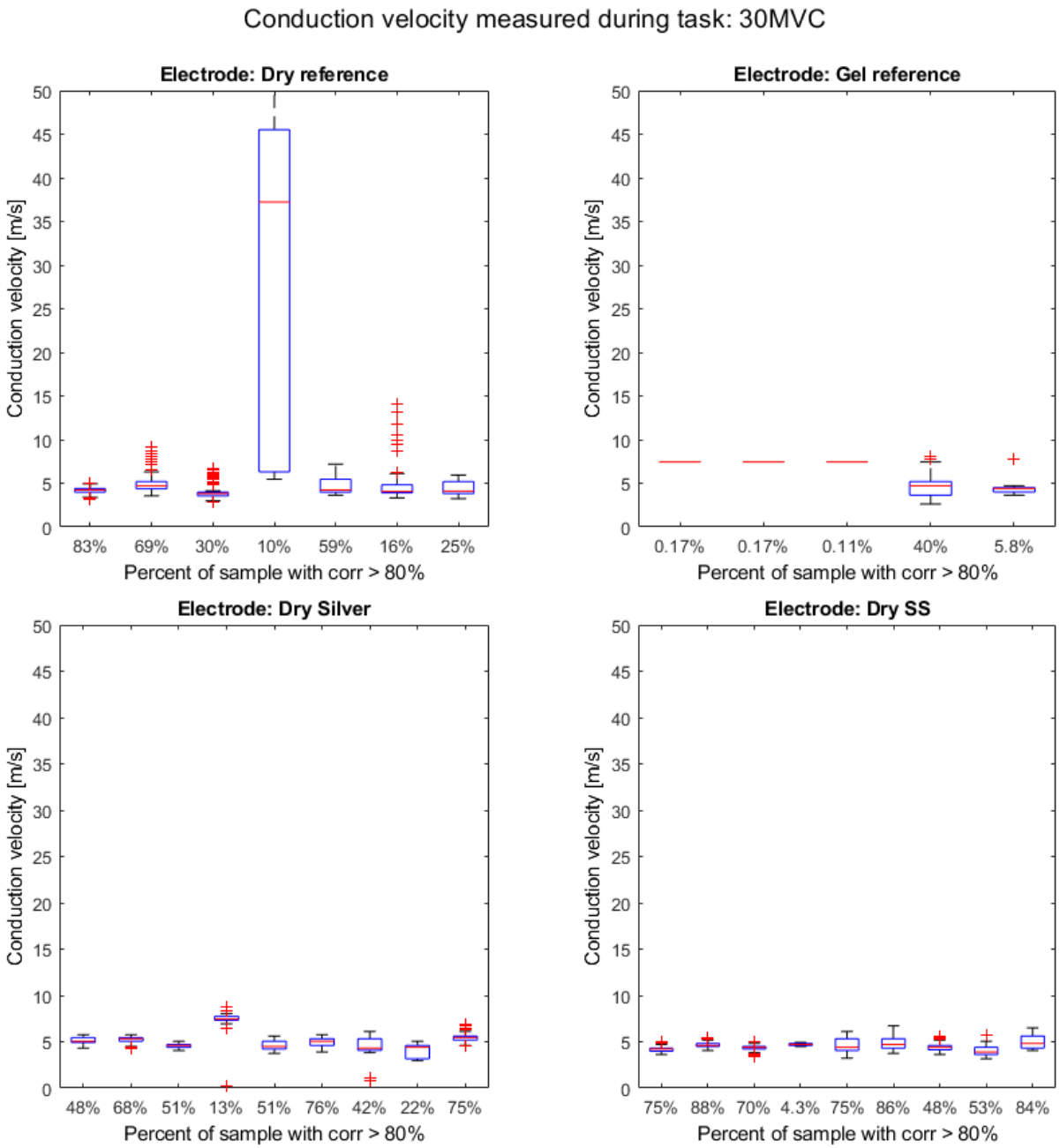

Figure 57: Conduction Velocity boxplot 30% MVC DD

Exercise 4: 50% MVC, Single differential

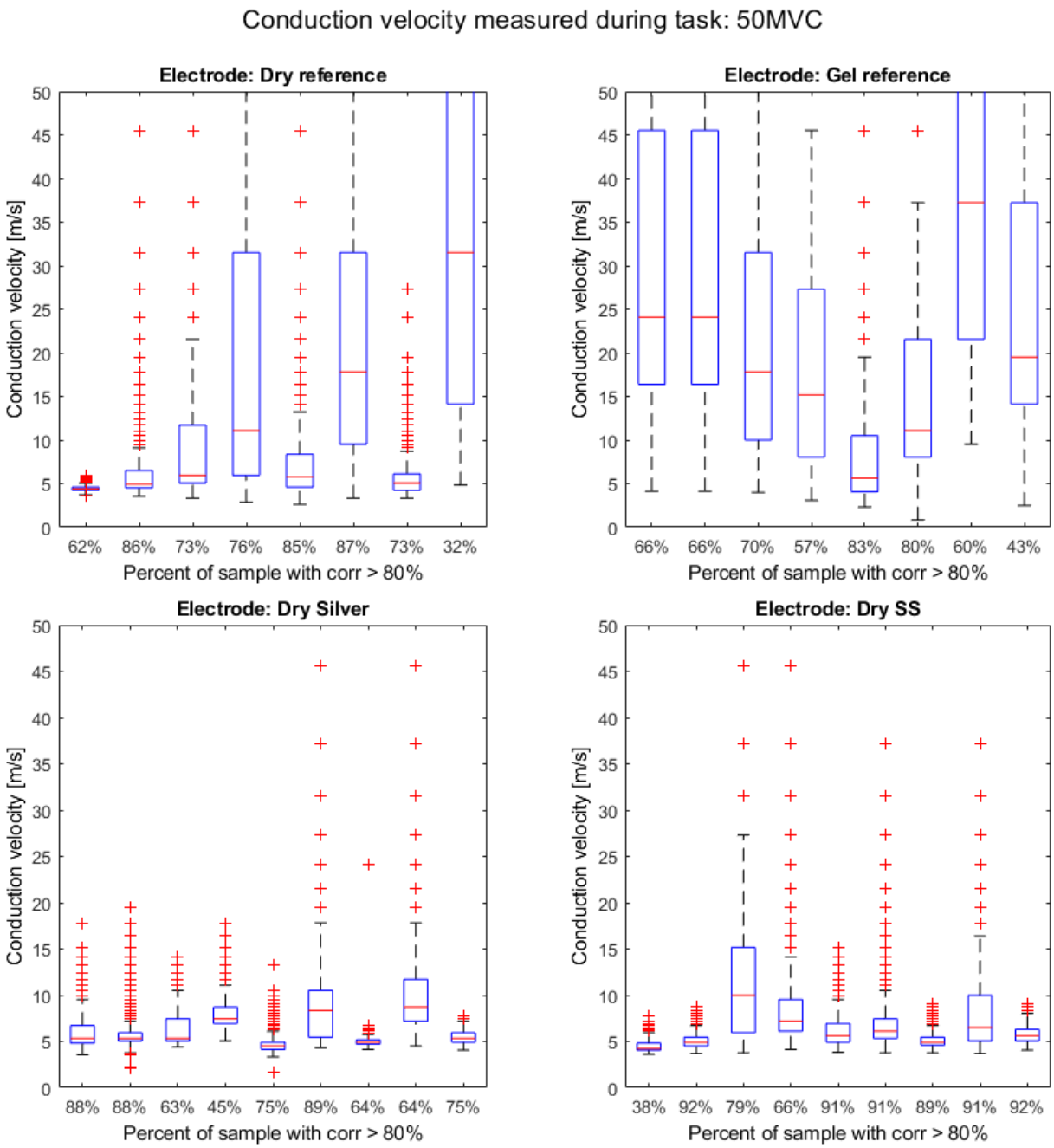

Figure 58: Conduction Velocity boxplot 50% MVC SD

Exercise 4: 50% MVC, Double differential

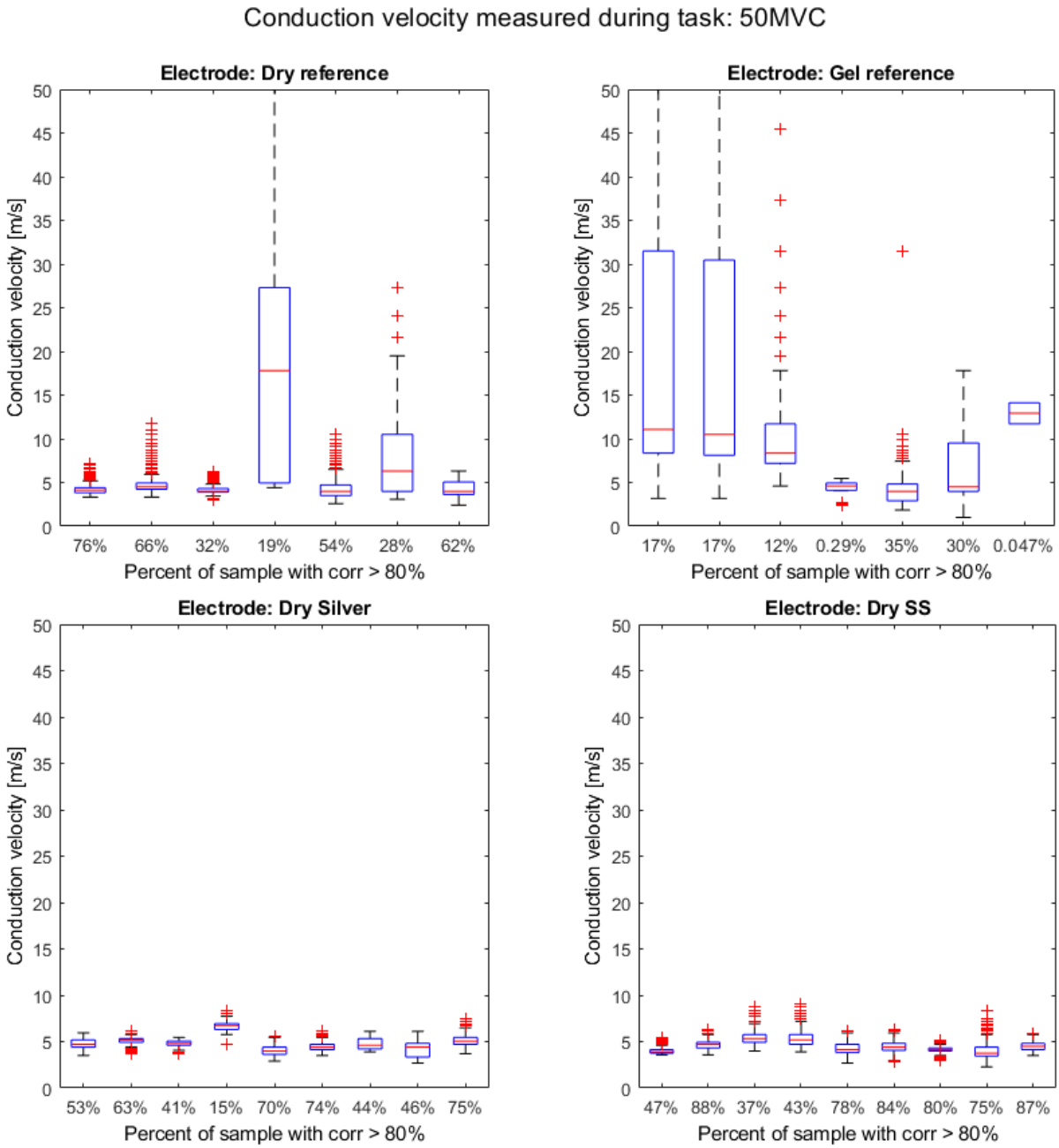

Figure 59: Conduction Velocity boxplot 50% MVC DD

4.5.2. Boxplots of Conduction Velocity results

Looking first at the single differential results, it can be observed a clear difference between the two first diagrams (corresponding to the BIOART array applied in dry skin and with gel) and silver and stainless steel prototypes. Although the percentage of samples with a high correlation is high in all cases and in all exercises except 10 MVC, the boxes spread a lot and out of the CV human range in the case of the first two diagrams. Focusing on silver and stainless steel, it can be seen medians close to the CV human range however some of them are not.

For the double differential results and only focusing on silver and stainless steel it's observed that the CV distribution values are very concentrated around their medians and all of them inside the expected range. The exercise with more difficulty to get high correlated samples is 10% MVC on the other side the exercise with higher number of correlated samples is 50% MVC.

Regarding the silver and the stainless steel array, a similar behavior is observed although in bigger number of occasions stainless steel has had higher number of high correlated samples.

4.6. Regression coefficients

This last section is focused on the 4th exercise 50% of MVC. In this particular exercise, that lasts up to 2 minutes, muscle ends up developing fatigue due the duration of the sustained contraction. For segments of time in this exercise the parameters of CV, MNF MDF and RMS were computed. Each of this parameters have a relation with the fatigue: CV, MNF, and MDF decrease while RMS increases when the muscle is fatigued.

In order to detect the trends in the 4th exercise of all these parameters during the exercise, a linear regression of each the parameters over time was performed. Linear regression fits a linear function relating the data. As an outcome, the slope of the linear regressions is depicted in the next graphs. A positive coefficient indicates a positive slope, therefore, an increase over time of that parameter, whereas a negative indicates a decrease over time.

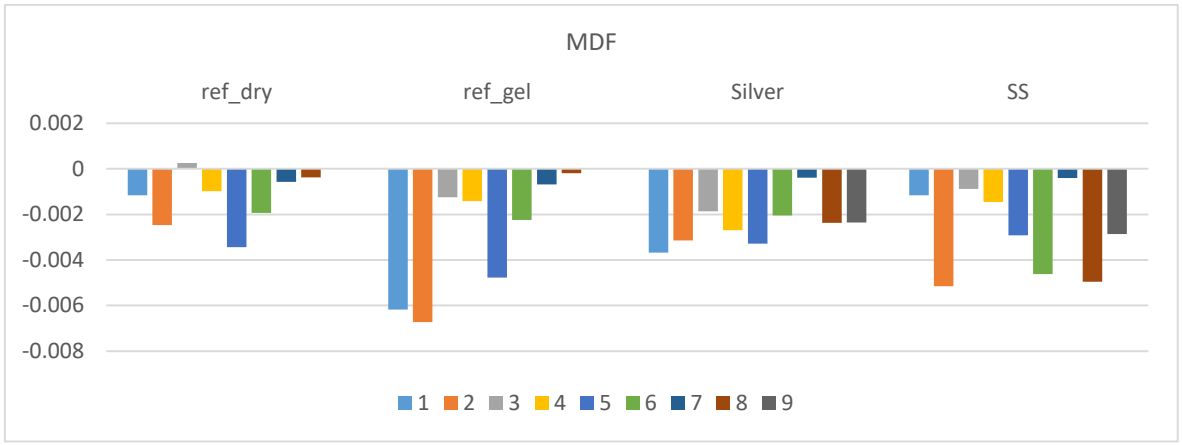

Figure 60: Regression coefficient, MDF

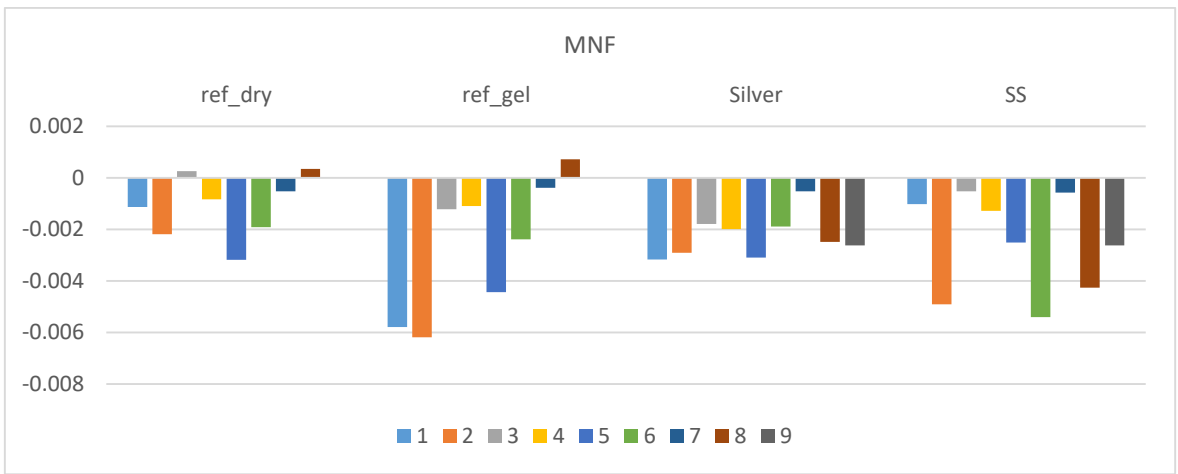

Figure 61: Regression coefficient, MNF

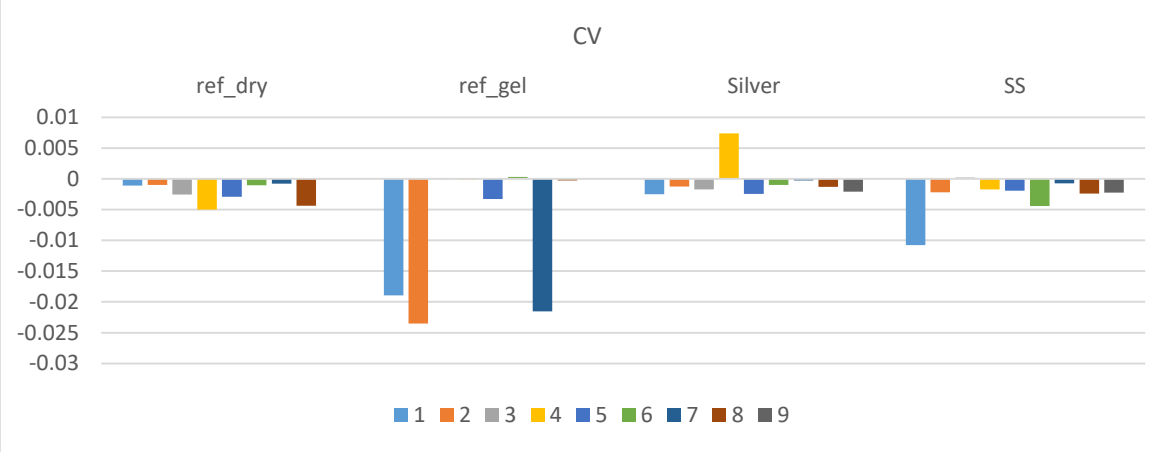

Figure 62: Regression coefficient, CV

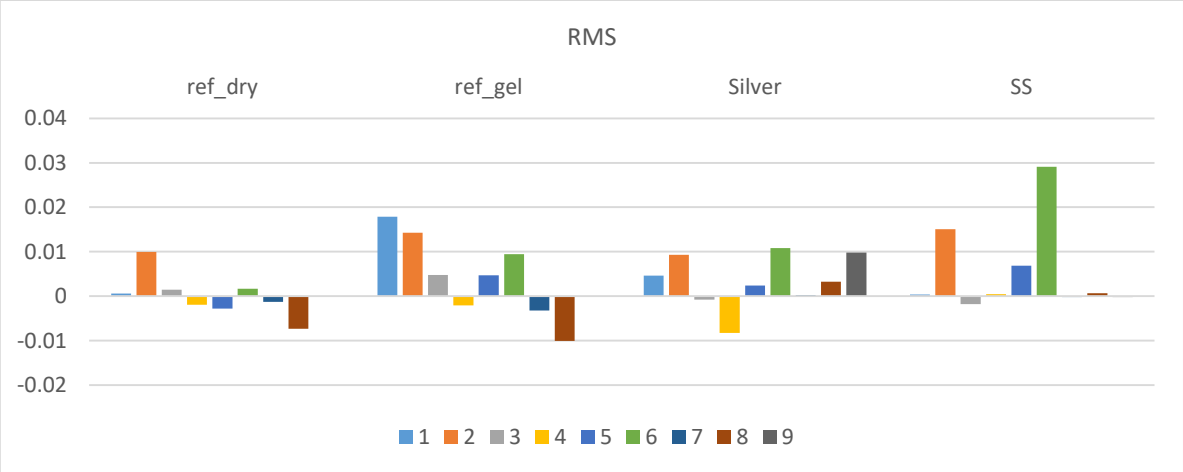

Figure 63: Regression coefficient, RMS

4.6.1. Regression coefficients results.

Starting with MDF and MNF, and once again focusing only in silver and stainless steel (last two), an expected decrease of this parameter is observed in all cases, negative slope and regression coefficient, in the case of silver the results appear to be more uniformly distributed and in the case of stainless steel more varying.

For the CV, the negative regression coefficients show a decrease over the time, there's a subject with a positive regression coefficient that doesn't follow the trend.

The most varying results and the less conclusive are depicted in the RMS graph showing a big number of subjects with positive regression coefficient, some of them close to 0 and the same subject that had a positive CV regression coefficient it shows here a negative regression coefficient in the evolution of the RMS value what seems to be opposite to the expected.

5. Conclusions and future development

The aim of this work was to evaluate the quality of low-cost and easy-to-use alternatives for electrode arrays in terms of EMG parameters that can be extracted from the recorded EMG signal. The motivation comes from the idea of using the HD-EMG technology outside of the research environment, in medical practice and in everyday life. To achieve this goal, the devices based on HD-EMG should be affordable and easy-to-use. Although the affordability is a relative term with respect to the application, e.g. the cost of a diagnosis tool based on HD-EMG and used in clinical centers can have several times higher price than consumer electronics intended for home use and leisure, but easy-to-use characteristic is of vital importance for usability. Currently, the use of HD-EMG implies manual application of conductive gel to each electrode. Considering that in some applications the number of electrodes can be several hundreds, the set-up process can take several hours, which is surely a limiting factor in practical use. Therefore, the main objective of this thesis was to evaluate the use of dry electrode alternatives in practical conditions with motivation to arrive to the plug-and-play HD-EMG solution.

Since it was not expected that these electrodes, especially when used without the conductive gel, could achieve comparable signal quality with commercial electrodes that use gel, the comparison with commercial electrodes was not performed. Instead, the electrodes were used to estimate the conduction velocity and muscle fatigue using the known and well-documented algorithms. The ability to estimate these parameters in a meaningful, expected, and physiologically viable range indicates the sufficient quality of the recording equipment.

Summing up the results acquired it's observable:

From the time series results, a clear visualization of the MUAP propagating along the channels with high correlation coefficient associated specially in the double differential recordings and consistent estimations of conduction velocity of both materials.

Regarding the spectra results, a normal power distribution in the expected range along the channels is observed in both materials.

In respect the bivariate analysis the performance in single differential approach seems to be reasonably similar. However, the number of samples with low correlation coefficient or out of the CV human range seems to be still high. On the contrary, double differential approach reduces effectively the number of samples with no physical meaning (out of human CV range).

Stainless steel shows in double differential a good performance and better compared to silver, the great majority of samples are concentrated in the high correlation and human expected range. This can be clearly observed in the 50% MVC DD of Stainless steel bivariate analysis.

The intensity analysis shows a similar result comparing silver and stainless steel in the all subject analysis the medians very close (almost aligned) and the variances very similar also so showing a reasonably similar behavior in this point.

The box plot analysis of conduction velocity and correlation shows extra info respect the bivariate analysis by adding the percentage of highly correlated samples and confirming once again very similar results both for silver and stainless steel.

The obtained results confirm that the low-cost alternatives to commercial electrode arrays without application of conductive gel, in particular stainless steel plates and silver-plated brass can be used to record EMG signal with sufficient quality to extract parameters for estimation of conduction velocity of muscle fibers and to estimate the muscle fatigue. This result indicates that the signal obtained using these electrodes is of sufficient quality to be used in the practical application.

Summarizing, the following points highlight some conclusions:

- Although not concluding the results show similar performances between these two materials.
- The results encourage the research in the possibility to use stainless steel as an alternative material for applications regarding surface electromyography.
- The applications could include medical purposes.

Next steps and future work encourage the research to move forward in reconfirm the results here exposed by investigating other aspects and trying to compare as well between these two materials including more subjects and different muscles to be applied. A related work could study the physical and electrical properties as it could be the impedance and its behavior over the skin and their response as it could be the motion artifact. Another step could be the use and test of the material in a new prototype designed for a specific purpose or application and establish indicators of the viability examples of this could be rehabilitation and robot control.

Bibliography

Asghari Oskoei, Mohammadreza, Huosheng Hu, and John Q. Gan. 2009. “Manifestation of Fatigue in Myoelectric Signals of Dynamic Contractions Produced during Playing PC Games.” in.

Ashley- Ross, Miriam A. 2005. “ Electromyography: Physiology, Engineering, and Noninvasive Applications . Edited by Roberto Merletti and , Philip Parker . IEEE Press. Hoboken (New Jersey): Wiley- Interscience. $99.95. Xxii + 494 p; Ill.; Index. ISBN: 0- 471- 67580- 6. 2004. .” *The Quarterly Review of Biology*.

Basmajian, J. V. and Carlo J. De Luca. 1985. “Chapter3: Description and Analysis of the EMG Signal.” in *Muscles alive: their functions revealed by electromyography*.

Cavalcanti Garcia, Ma and TM M. Vieira. 2011. “Surface Electromyography: Why, When and How to Use It.” *Rev Andal Med Deporte. Rev Andal Med Deporte. Rev Andal Med Deporte*.

Danielle Moores and Erica Cirino. 2016. “Electromyography (EMG): Purpose, Procedure, and Results.” Retrieved March 4, 2019 (https://www.healthline.com/health/electromyography).

Day, By Scott. 2004. *Important Factors in Surface EMG Measurement*.

Van Dijk, Ludger, Corry K. Van Der Sluis, Hylke W. Van Dijk, and Raoul M. Bongers. 2016. “Learning an EMG Controlled Game: Task-Specific Adaptations and Transfer.” *PLoS ONE*.

Holobar, Ale, Marco Alessandro Minetto, Alberto Botter, Francesco Negro, and Dario Farina. 2010. “Experimental Analysis of Accuracy in the Identification of Motor Unit Spike Trains from High-Density Surface EMG.” *IEEE Transactions on Neural Systems and Rehabilitation Engineering*.

Holobar, Aleš and Damjan Zazula. 2007. “Multichannel Blind Source Separation Using Convolution Kernel Compensation.” *IEEE Transactions on Signal Processing*.

Kazamel, Mohamed and Paula Province Warren. 2017. “History of Electromyography and Nerve Conduction Studies: A Tribute to the Founding Fathers.” *Journal of Clinical Neuroscience*.

Knaflitz, M., R. Merletti, and C. J. De Luca. 2017. “Inference of Motor Unit Recruitment Order in Voluntary and Electrically Elicited Contractions.” *Journal of Applied Physiology*.

Li, Guanglin, Aimee E. Schultz, and Todd A. Kuiken. 2010. “Quantifying Pattern Recognition- Based Myoelectric Control of Multifunctional Transradial Prostheses.” *IEEE Transactions on Neural Systems and Rehabilitation Engineering*.

Limsakul, Chusak, Huosheng Hu, Angkoon Phinyomark, Pornchai Phukpattaranont, and Sirinee Thongpanja. 2012. “The Usefulness of Mean and Median Frequencies in Electromyography Analysis.” in *Computational Intelligence in Electromyography Analysis - A Perspective on Current Applications and Future Challenges*.

Luca, Carlo J. De. 2002. “Surface Eectromyography : Detection and Recording.” *Delsys Incorporated*.

Manolakis, Dg, Vk Ingle, and Sm Kogon. 2000. *Statistical and Adaptive Signal Processing: Spectral Estimation, Signal Modeling, Adaptive Filtering, and Array Processing*.

Marchal-Crespo, Laura and David J. Reinkensmeyer. 2009. “Review of Control Strategies

for Robotic Movement Training after Neurologic Injury.” *Journal of NeuroEngineering and Rehabilitation*.

Merletti, Roberto and Dario Farina. 2016. *Surface Electromyography: Physiology, Engineering and Applications*.

Petrofsky, Jerrold Scott, Roger M. Glaser, and Chandler A. Phillips. 1982. “Evaluation of the Amplitude Aud Frequency Components of the Surface Emg as an Index of Muscle Fatigue.” *Ergonomics*.

Rojas-Martínez, Monica, Miguel A. Mañanas, and Joan F. Alonso. 2012. “High-Density Surface EMG Maps from Upper-Arm and Forearm Muscles.” *Journal of NeuroEngineering and Rehabilitation*.

Staudenmann, Didier, Jaap H. van Dieën, Dick F. Stegeman, and Roger M. Enoka. 2013. “Increase in Heterogeneity of Biceps Brachii Activation during Isometric Submaximal Fatiguing Contractions: A Multichannel Surface EMG Study.” *Journal of Neurophysiology*.

Strang, Eric P. Widmaier; Hershel Raff; and Kevin T. 2013. “Vander’s Human Physiology.” in *Vander’s Human Physiology The mechanisms of body fuction*.

Vaca Benitez, Luis Manuel, Marc Tabie, Niels Will, Steffen Schmidt, Mathias Jordan, and Elsa Andrea Kirchner. 2013. “Exoskeleton Technology in Rehabilitation: Towards an EMG-Based Orthosis System for Upper Limb Neuromotor Rehabilitation.” *Journal of Robotics*.

Verikas, Antanas, Evaldas Vaiciukynas, Adas Gelzinis, James Parker, and M. Charlotte Olsson. 2016. “Electromyographic Patterns during Golf Swing: Activation Sequence Profiling and Prediction of Shot Effectiveness.” *Sensors (Switzerland)*.

Vieira, Taian M. M., Roberto Merletti, and Luca Mesin. 2010. “Automatic Segmentation of Surface EMG Images: Improving the Estimation of Neuromuscular Activity.” *Journal of Biomechanics*.

Appendices

Parameters processing Matlab Script:

```
%% PROCESSING %%

close all
clear all
colordef none


subject_name = {'Sujeto_1', 'Sujeto_2',
'Sujeto_3','Sujeto_4','Sujeto_5','Sujeto_6','Sujeto_7','Sujeto_8','Sujet
o_9'};
task_name = {'_100MVC_A', '_10MVC_A', '_30MVC_A','_50MVC_fatigue'};
electrode_name =
{'Dry_reference','Gel_reference','Dry_Silver','Dry_SS'};



fs = 2048;              % sampling rate (tasa de muestreo)
IED = 1e-2;
interp_fact_CV = 10;
fs_CV = fs*interp_fact_CV;

info_SNR= [];
info_MNF = [];
info_MDF = [];
info_CV = [];
info_R = [];
info_Spectrum = [];
final_data=[];

for subject = 1:8
    for task = 1:4
        for electrode=1:4

            file = [pwd, '\signals\', subject_name{subject}, '\',
electrode_name{electrode},task_name{task}, '.mat'];
            if not(isfile(file)), continue; end
            load(file)
            var1 = Data;

            display(['Processing: ', subject_name{subject}, ', ',
task_name{task}, ', ', electrode_name{electrode}])


            if (electrode==1 || electrode==2)
                if(size(var1,2)>28)
                    var1(:,[6,12,18,24,30,31,32]) = [];
                else
                    var1(:,[6,12,18,24]) = [];
                end
            else
                var1(:, [5,10,15,20:end])=[];
            end

            emg = var1;
            nchan = size(emg,2);
```

```
            if nchan==16, nrow = 4; else nrow=5; end
            ncol = nchan/nrow;


            times_file = [pwd, '\signals\', subject_name{subject}, '\',
electrode_name{electrode},task_name{task}, '.txt'];
            times = dlmread(times_file);
            t_start = times(1);
            t_end = times(2);

            %---------------------------------------------------------
---------------
            %                         Use Double differential signals
            %---------------------------------------------------------
---------------
            emg = diff(emg,1,2);
            eliminate = nrow:nrow:nchan-1;
            emg(:,eliminate) = [];

            nrow = nrow-1;
            nchan = nrow*ncol;


%=========================================================================
===
            %                                 Filtering
%=========================================================================
===
            %---------------------------------------------------------
---------------
            %                                 Band Pass
            %---------------------------------------------------------
---------------
            [b,a] = butter(3,[15 350]/(fs/2));
            x_filt= filtfilt(b,a, emg);

            %---------------------------------------------------------
---------------
            %                             Notch Filter
            %---------------------------------------------------------
---------------
            Fnotch = 50;             % notch frequency
            wo = Fnotch/(fs/2);  bw = wo/50;
            [b,a] = iirnotch(wo,bw);
            x_filt = filtfilt(b,a, x_filt);

            Fnotch = 150;             % notch frequency; third harmonic
            wo = Fnotch/(fs/2);  bw = wo/50;
            [b,a] = iirnotch(wo,bw);
            x_filt = filtfilt(b,a, x_filt);



%=========================================================================
===
            %                         Extraction of Measures
```

```
%=========================================================================
===
            %-------------------------------------------------------------
---------------
            %                                   SNR
            %-------------------------------------------------------------
---------------

            x_noise = x_filt(516:t_start, :); % don't start from the
beginning
            x_signal = x_filt(t_start:t_start+length(x_noise)-1, :);

            SNR = nan(1,25);
            for i = 1:nchan
                SNR(i) = snr(x_signal(:,i), x_noise(:,i));
            end


            %-------------------------------------------------------------
---------------
            %                          Windowing and PSD estimation
            %-------------------------------------------------------------
---------------
            % be careful when changing length of x1 because dimension of
            % pwelch depends on it
            Lw = floor(0.5*fs); %(s) ancho de la ventana
            step = floor(0.25*fs);
            Lt = t_end-t_start+1;
            t_step = 0:step/fs:(Lt-Lw)/fs;

            x = x_filt(t_start :t_end, :);

            MNF = [];
            MDF = [];
            CV=[];
            R=[];
            Spectrum = [];

            % Windowing
            for  t_aux = 1: step: (Lt-Lw)

                MNF_aux = nan(1,25);
                MDF_aux = nan(1,25);
                CV_aux = nan(1,25);
                R_aux = nan(1,25);
                Spectrum_aux = [];

                x_win = x(t_aux:t_aux+Lw-1, :);

                CV_index = 0;
                for chan=1:nchan

                    Spectrum_aux_ch = [];
                    [P, f] = pwelch(x_win(:, chan), 256, 128, 512);
                    f = f/pi*(fs/2);
                    Spectrum_aux_ch = P;
%                     plot(f,P);
%                     Spectrum_aux = P;
```

```
                    %-------------------------------------------------
-----------------------
                    %                               Mean Frequency
                    %-------------------------------------------------
-----------------------
                    MNF_aux(chan)= (f'*P)/sum(P);

                    %-------------------------------------------------
-----------------------
                    %                             Median Frequency
                    %-------------------------------------------------
-----------------------
                    P_total = sum(P);
                    P_cum = cumsum(P);
                    MDF_aux(chan) = f(find(P_cum>P_total/2,1));

                    %-------------------------------------------------
-----------------------
                    %                             Conduction velocity
                    %-------------------------------------------------
-----------------------
                    if mod(chan, nrow) % make sure you calculate CV only
if
                                       % of channels in the same row
                    CV_index = CV_index+1;
                    dvisual1 = x_win(:,chan);
                    dvisual2 = x_win(:,chan+1);
                    [r1,lags1] = xcorr(dvisual2,dvisual1,'coeff');
                    t1_cor=1:length(r1);
                    t2_cor=1:(1/interp_fact_CV):length(r1);
                    r1=interp1(t1_cor,r1,t2_cor,'spline');
                    re = r1;
                    k=length(r1)/2; %Center of the vector
                    [R_max,I] = max(r1);
                    dephase_samp = abs(k-I);
                    CV_aux(CV_index) = IED/(dephase_samp/fs_CV);
                    R_aux(CV_index) = R_max;
                    end
                    Spectrum_aux(:,:,chan) = Spectrum_aux_ch;
                end

                MNF = [MNF; MNF_aux];
                MDF = [MDF; MDF_aux];
                CV = [CV; CV_aux];
                R = [R; R_aux];
                Spectrum = [Spectrum; Spectrum_aux];
            end

            info_SNR= [info_SNR;subject,task,electrode, SNR];
            info_MNF =
[info_MNF;repmat([subject,task,electrode],size(MNF,1),1),MNF];
            info_MDF =
[info_MDF;repmat([subject,task,electrode],size(MDF,1),1),MDF];
            info_CV =
[info_CV;repmat([subject,task,electrode],size(CV,1),1),CV];
            info_R =
[info_R;repmat([subject,task,electrode],size(R,1),1),R];
            info_Spectrum =
[info_Spectrum;repmat([subject,task,electrode],size(Spectrum,1),1),Spect
rum];
```

```
        end
    end
end


filename = 'info_DD.mat';
save(filename,'info_SNR','info_MNF','info_MDF','info_CV','info_R')
fprintf(1,'Proceso Terminado')
```